

ON AXISYMMETRIC TRAVELING WAVES  
AND RADIAL SOLUTIONS OF  
SEMI-LINEAR ELLIPTIC EQUATIONS

THOMAS P. WITELSKI  
Department of Mathematics  
Duke University  
Durham, NC 27708-0320  
*E-mail:* [witelski@math.duke.edu](mailto:witelski@math.duke.edu)

KINYA ONO  
Department of Mathematics  
Boston University  
Boston, MA 02215  
*E-mail:* [ono@math.bu.edu](mailto:ono@math.bu.edu)

TASSO J. KAPER  
Dept. of Mathematics and Center for BioDynamics  
Boston University  
111 Cummington Street  
Boston, MA 02215  
*E-mail:* [tasso@math.bu.edu](mailto:tasso@math.bu.edu)

**ABSTRACT.** Combining analytical techniques from perturbation methods and dynamical systems theory, we present an elementary approach to the detailed construction of axisymmetric diffusive interfaces in semi-linear elliptic equations. Solutions of the resulting non-autonomous radial differential equations can be expressed in terms of a slowly varying phase plane system. Special analytical results for the phase plane system are used to produce closed-form solutions for the asymptotic forms of the curved front solutions. These axisymmetric solutions are fundamental examples of more general curved fronts that arise in a wide variety of scientific fields, and we extensively discuss a number of them, with a particular emphasis on connections to geometric models for the motion of interfaces. Related classical results for traveling waves in one-dimensional problems are also reviewed briefly. Many of the results contained in this article are known, and in presenting known results, it is intended that this article be expository in nature, providing elementary demonstrations of some of the central dynamical phenomena and mathematical techniques. It is hoped that the article serves as one possible avenue of entree to the literature on radially symmetric solutions of semilinear elliptic problems, especially to those articles in which more advanced mathematical theory is developed.

**1. Introduction.** In a wide variety of scientific fields, including chemical physics (Borgis and Moreau [1988], Witelski et al. [1998]), combustion theory (Fife [1988], Volpert et al. [1994]), reaction-diffusion problems (Grindrod [1996]), fluid mechanics (Lamb [1993], Majda and Bertozzi [1999]), population dynamics (Murray [1990]), and mathematical biology (Keener and Sneyd [1998], Murray [1990]), to name but a few, problems describing the formation of spatial structure involve the analysis of localized transition layers or diffusive interfaces. These interfaces are boundaries that separate regions of spatially uniform homogeneous solutions of the nonlinear systems. The form of the governing equations in these problems determines the details of the local structure of the transition layers, as well as their motion and their stability. The long-time asymptotic state of the system is ultimately determined by the motion and interaction of these localized structures, and possible outcomes include complex patterns (Goldstein et al. [1996], Grindrod [1996], Murray [1990]) and rotating spiral structures (Bernoff [1991], Tyson and Keener [1988]). There are extensive bodies of mathematical literature examining existence, uniqueness, stability and dynamics of such problems in applications in reaction-diffusion systems, fluid dynamics, reactive-transport phenomena, and other areas of applied physics; as an introduction to this field, we cite the following incomplete list of some of the fundamental earlier works and some of the more recent reviews (Aronson and Weinberger [1978], Berestycki and Lions [1980], Brezis and Lieb [1984], Fife [1988], Gidas et al. [1979], Jones [1983b], Kaper and Kwong [1988], Kerner and Osipov [1994], Kuzin and Pohozaev [1997], McLeod and Serrin [1968] and [1987], Ni [1988], Powell [1997], Terman [1987], Vasileva et al. [1995]).

In this article we review, from an elementary point of view, some of the results for problems in the study of nonlinear reaction-diffusion problems and their equilibria, corresponding to solutions of nonlinear elliptic problems. Combining analytical techniques from dynamical systems theory (Guckenheimer and Holmes [1983]), perturbation methods (Kevorkian and Cole [1996]), and from the study of motion of diffusive interfaces (Fife [1988]), we present a detailed construction of radially symmetric curved fronts, see Figure 1. Asymptotic and explicit formulae are given for the positions of the fronts and their wavespeeds. We also discuss how these simple solutions can serve as the fundamental building blocks for problems in more complicated geometries that are

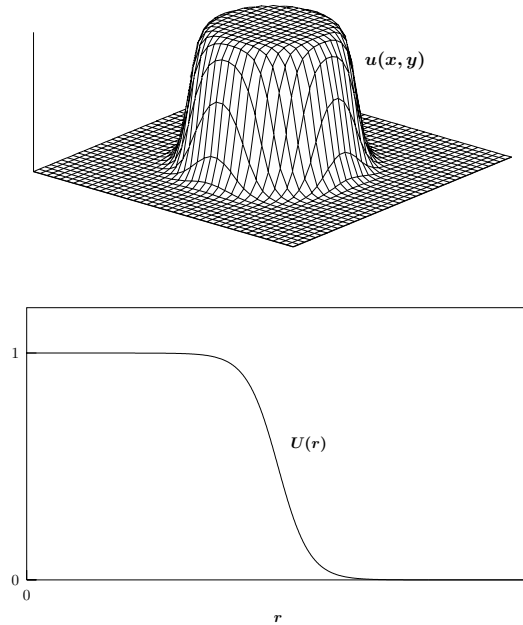


FIGURE 1. A two-dimensional localized axisymmetric solution of the semi-linear elliptic equation (1.2) and its radial profile,  $u = U(r)$ .

often studied using more advanced techniques.

We will make use of the simplest model that qualitatively describes the behavior of localized transition layers. The equation we will analyze is the nonlinear second order differential equation:

$$(1.1) \quad \frac{d^2U}{dz^2} + c \frac{dU}{dz} + F(U; \omega) = 0,$$

where  $c$  is a damping parameter describing the level of dissipation in the system and  $\omega$  is a control parameter modifying the form of the nonlinear function  $F(U; \omega)$ .  $F(U; \omega)$  is a cubic-like, or *bi-stable*, function of  $U$ , see Figure 2a. Bistability implies that there is a well-defined range of values,  $\omega_{\min} < \omega < \omega_{\max}$ , such that  $F(U; \omega)$  has three real roots, see Figure 2a, and for  $\omega$  outside of this range,  $F$  has only one real root. For every  $\omega \in (\omega_{\min}, \omega_{\max})$ , equation (1.1) has three equilibrium solutions, and we label these  $U^L(\omega) < U^M(\omega) < U^R(\omega)$ , corresponding to the three roots of  $F(U; \omega)$ .

Motivated by problems from the disciplines cited above and by earlier analytical studies, we examine problems in which the bistable function  $F(U; \omega)$  is the sum of a term with linear dependence on a control parameter  $\omega$  and a fixed nonmonotone function  $f(U)$ ,

$$(1.2) \quad F(U; \omega) = f(U) - \omega U,$$

where  $f(U) = o(U)$  as  $U \rightarrow 0$ . For example, in the study of first order phase transitions,  $f(U)$  is called the free energy density and  $\omega$  is a measure of the temperature in the system (Chan [1977]). With this choice for the form of  $F(U; \omega)$ , the trivial state  $U^L = 0$  is a homogeneous solution for all values of  $\omega$ .

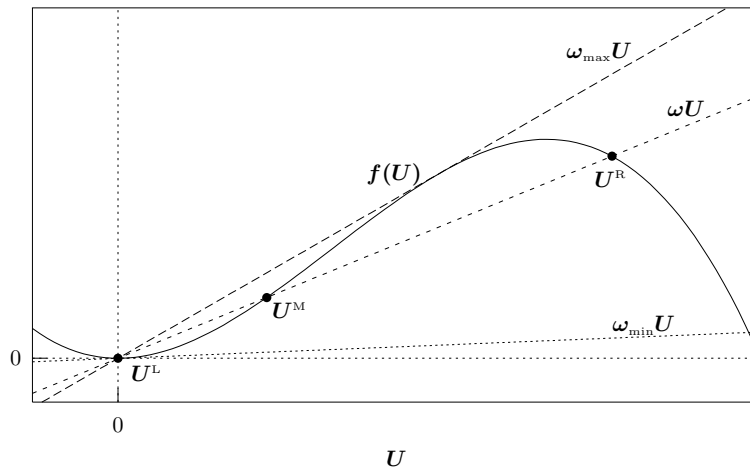
As an ordinary differential equation, the system (1.1) may be interpreted as a damped anharmonic oscillator (Goldstein [1980]), with the damping parameter  $c$  describing the level of dissipation of the motion and the force  $F$  being derived from a nonconvex inverted double-well potential energy function  $\mathcal{V}(U)$ , see Figure 2b,

$$(1.3) \quad F(U; \omega) = \frac{\partial \mathcal{V}}{\partial U}.$$

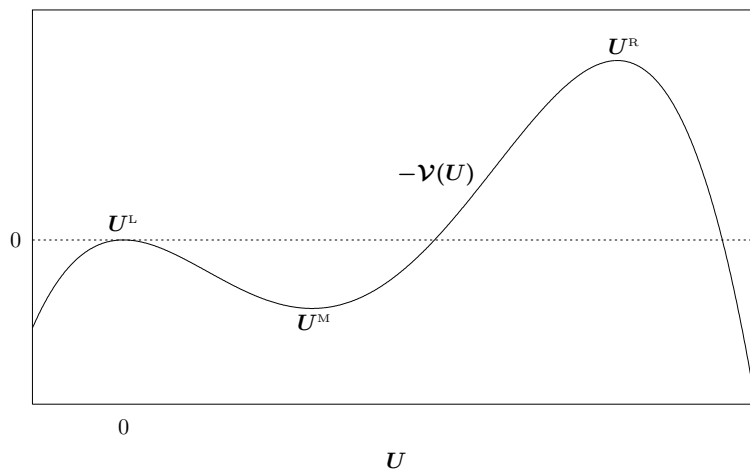
To uniquely specify the potential, we define its value at the point  $U = U^L$  as  $\mathcal{V}(U^L) = 0$ . In terms of the inverted double well potential  $\mathcal{V}(U)$ ,  $U^L$  and  $U^R$  are maxima while  $U^M$  is a local minimum. The value of  $\omega$  determines the relative heights of the maxima. We will show that for an appropriate level of damping  $c$ , dissipation can exactly balance the difference in potential heights to yield a unique bounded solution connecting  $U^L$  and  $U^R$ . This solution is called a heteroclinic orbit, and it is the solution of (1.1) that describes the structure of diffusive interfaces. We now review some applications that depend upon this model.

Equation (1.1) arises directly from the description of planar traveling wave solutions of reaction-diffusion equations. For example, consider the FitzHugh-Nagumo equations for the propagation of electrical impulses in nerve cells from mathematical biology (Grindrod [1996], Murray [1990])

$$(1.4) \quad \frac{\partial u}{\partial t} = \frac{\partial^2 u}{\partial x^2} + f(u) - \omega u, \quad \frac{\partial \omega}{\partial t} = \varepsilon u.$$



(a)



(b)

FIGURE 2. (a) Construction of the zeroes of  $F(U; \omega) = f(U) - \omega U$ . (b) The inverted double well potential  $\mathcal{V}(U)$ .

In the limit that  $\varepsilon \rightarrow 0$ , this problem is a singular perturbation problem for a relaxation oscillator. For  $\varepsilon = 0$ , the two equations decouple, and one can seek traveling wave solutions in the form  $u(x, t) = U(x - ct)$ , where  $U(z)$  is given by the solution of (1.1), see McKean [1970]. More generally, in the study, in several dimensions, of scalar reaction-diffusion equations, also called Alan-Cahn models (Taylor and Cahn [1994]),

$$(1.5) \quad \frac{\partial u}{\partial t} = \nabla^2 u + F(u; \omega),$$

one also finds one-dimensional planar fronts of the form  $u(\mathbf{x}, t) = U(\mathbf{k} \cdot \mathbf{x} - ct)$ . This model appears in many classical studies of the propagation of phase transitions in time-dependent Ginzburg-Landau problems (Dixon et al. [1991]). For different forms of the nonlinear function  $F(u; \omega)$ , (1.1) has been used in population genetics to study the spread of a favored trait, originally given by Fisher's equation (Murray [1990]). In all of these problems, solutions of the partial differential equation exist whose spatial structure is given by the solution of (1.1) and the speed of propagation  $c$  is determined by a balance of nonlinear and dissipative effects in the ordinary differential equation. Analytical determination of the speed of propagation in closed form has been studied extensively for classes of polynomial nonlinearities  $F(U; \omega)$  (Benguria and Depassier [1994], Dixon et al. [1991], Powell and Tabor [1992]). However, some open questions still remain regarding the calculation of  $c$  for more general problems (Goriely [1995], Cisternas and Depassier [1996]).

Nontrivial equilibrium solutions of (1.5) have also been the focus of much study (Ni [1988]). The bistable reaction-diffusion equation (1.5) is also the basis for nucleation theory, describing the formation and growth of spatial inhomogeneities in chemical reactions. In this setting, small initial perturbations in a uniform reactive medium can grow to become nucleation centers, the sources of larger scale pattern formation. Finite-size equilibrium nuclei satisfy the steady-state equation

$$(1.6) \quad \nabla^2 u + F(u; \omega) = 0,$$

sometimes called the scalar field equation (Ni [1988]).

Another application where semilinear elliptic equations of the form (1.6) occur is in the study of incompressible fluid dynamics. The two-dimensional vorticity-streamfunction form of the Euler equations for

incompressible inviscid flow can be written as (Lamb [1993], Majda and Bertozzi [1999])

$$(1.7) \quad \frac{\partial \Omega}{\partial t} + \hat{\mathbf{k}} \cdot (\nabla \Psi \times \nabla(\nabla^2 \Psi)) = 0,$$

where  $\Psi = \Psi(x, y)$  is a streamfunction. If the Laplacian of the streamfunction is only a function of  $\Psi$ ,  $\nabla^2 \Psi = -F(\Psi)$ , then the cross product vanishes,  $\nabla \Psi \times F'(\Psi) \nabla \Psi = \mathbf{0}$ , and  $\Psi$  is a steady solution of the Euler equation (1.7) for any function  $F(\Psi)$ . Localized axisymmetric solutions of this problem represent vortex flows with zero total vorticity and are commonly called *eddies*.

Similarly, in chemical physics, nonlinear elliptic equations occur as mean field models to describe density functions. In Witelski et al. [1998], a semilinear elliptic equation (1.2) was derived for the density function of the spherically symmetric globule state of a collapse polymer chain. In this context, the problem is stated as an eigenvalue problem for a nonlinear elliptic problem:

$$(1.8) \quad \mathcal{H}[\psi] = \omega \psi, \quad \psi(\mathbf{x} \rightarrow \infty) \rightarrow 0, \quad \mathcal{H}[\psi] \equiv \nabla^2 \psi + f(\psi),$$

where  $\omega$  gives a measure of the potential energy of the solution.

It is well known that positive solutions of (1.6) must be radially symmetric (Gidas et al. [1979]). Therefore, we write  $u(\mathbf{x}) = U(r)$  and write the reduced form of the radial Laplacian operator in  $n$  dimensions,

$$(1.9) \quad \nabla^2 \equiv \frac{1}{r^{n-1}} \frac{d}{dr} \left( r^{n-1} \frac{d}{dr} \right) = \frac{d^2}{dr^2} + \frac{n-1}{r} \frac{d}{dr};$$

consequently, radially symmetric solutions of (1.6) satisfy the ordinary differential equation

$$(1.10) \quad \frac{d^2 U}{dr^2} + \frac{n-1}{r} \frac{dU}{dr} + F(U; \omega) = 0.$$

We note that equation (1.10) has the same qualitative structure as (1.1); it is a second order differential equation with linear damping and nonlinearity  $F(U; \omega)$ . However, there are some important technical differences between the two equations. While (1.1) is an autonomous

equation defined on  $-\infty < z < \infty$ , (1.10) is a nonautonomous equation defined on  $0 \leq r < \infty$ .

We will go on to demonstrate how the solution of the nonautonomous equation (1.10) can be related to the solution of (1.1) using perturbation methods. In Section 2 we discuss the basic properties of equation (1.1) in the phase plane. In Section 3 we will outline the properties of the nonautonomous radial equation (1.10). In Section 4 we use an autonomous approximation to reduce the radial problem to the form (1.1). In Section 5 we justify the use of (1.1) for the solution of (1.10) through a perturbation expansion that reduces the radial problem to a series of phase plane problems with slowly varying coefficients. In Section 6 we study a threshold effect by studying the instability of these radial solutions for time dependent reaction-diffusion equations. In Section 7 we review transversality arguments from dynamical systems theory for the analysis of the heteroclinic interface solution. Finally, in Section 8 we summarize the scope of our examination of this topic, and we describe briefly how the results have been extended, as well as how they can be used to construct more general curved front solutions.

**2. The autonomous problem.** In this section we review the classical phase plane analysis of the autonomous differential equation:

$$(2.1) \quad \frac{d^2U}{dz^2} + c \frac{dU}{dz} + F(U; \omega) = 0,$$

and we review some of its exact solutions. As described above, this equation has been studied extensively in the literature in connection with the structure of planar front traveling wave solutions.

**2.1. Phase plane analysis.** Equation (2.1) can be written as a system of first-order differential equations in the form

$$(2.2) \quad \frac{dU}{dz} = V, \quad \frac{dV}{dz} = -F(U; \omega) - cV.$$

To determine the local behavior near the equilibria,  $\{(U^E, 0) | U^E = U^L, U^M, U^R\}$ , we compute the Jacobian of vector field (2.2),

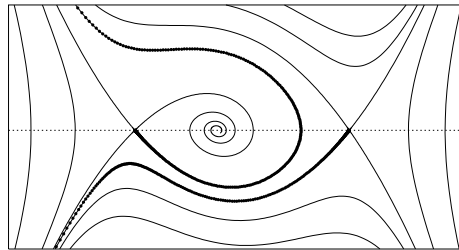
$$(2.3) \quad J = \begin{pmatrix} 0 & 1 \\ \omega - f'(U) & -c \end{pmatrix}$$

as part of a local stability analysis (Guckenheimer and Holmes [1983]). The eigenvalues of the Jacobian matrix at the equilibria  $(U^E, 0)$  are:

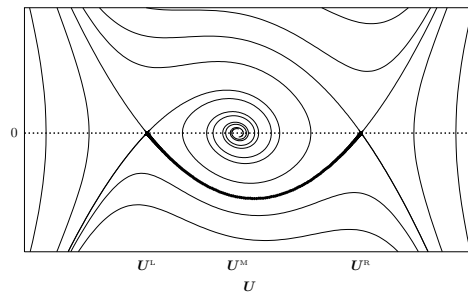
$$(2.4) \quad \lambda_{\pm}^E = \frac{-c \pm \sqrt{c^2 + 4\omega - 4f'(U^E)}}{2}, \quad U^E = \{U^R, U^M, U^L\}.$$

Hence for our bistable function  $F(U; \omega)$ ,  $(U^L, 0)$  and  $(U^R, 0)$  are saddle points, while  $(U^M, 0)$  is a spiral sink for  $c > 0$  (and is a center for  $c = 0$ ).

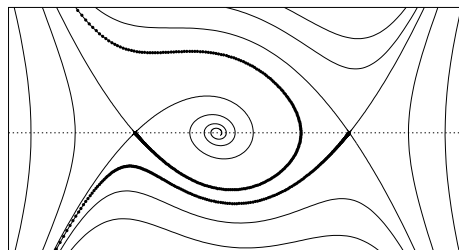
The heteroclinic orbit is the only monotone solution  $U = U(z)$  that is bounded for all  $-\infty < z < \infty$ . The heteroclinic orbit connecting the two maxima in (2.3) is not a structurally stable property of the system. Existence of the heteroclinic solution requires a special balance between the nonlinear and dissipative terms, see Fife and McLeod [1981] for a uniqueness result. This result implies the existence of a unique functional relationship between the parameters necessary for a heteroclinic connection,  $c = c(\omega)$ . For every value  $\omega \in (\omega_{\min}, \omega_{\max})$  we can define the local stable and unstable manifolds (Guckenheimer and Holmes [1983]) of the saddle points  $(U^L, 0)$  and  $(U^R, 0)$  that are involved in the construction of the heteroclinic orbit. The local stable manifold of  $(U^L, 0)$  is the set of initial conditions in a neighborhood of  $(U^L, 0)$  that stay in the neighborhood for all  $z > z_0$ , for some  $z_0$ , and that approach the equilibrium,  $U(z \rightarrow \infty) \rightarrow U^L$ , as  $z \rightarrow \infty$ . Linearized analysis shows that solutions on the local stable manifold approach  $(U^L, 0)$  tangent to the eigenvector corresponding to the stable eigenvalue  $\lambda_-^L < 0$ . Similarly, the local unstable manifold of  $(U^R, 0)$  is the set of all initial conditions in a neighborhood of that point that stay in the neighborhood for all  $z < z_0$ , for some  $z_0$ , and that approach  $(U^R, 0)$  exponentially in backward time, i.e.,  $U(z \rightarrow -\infty) \rightarrow U^R$  as  $z \rightarrow -\infty$ . Solutions on this manifold approach the equilibrium  $(U^R, 0)$  tangent to the eigenvector corresponding to the unstable  $\lambda_+^R > 0$  eigenvalue. Figure 3 shows the three possible relations between these two manifolds for different values of the parameters  $c, \omega$ ; (a) the stable manifold of  $(U^L, 0)$  lies above the unstable manifold of  $(U^R, 0)$ , (b) the two manifolds coincide, and the orbits lying in them are heteroclinic connections from  $(U^R, 0)$  to  $(U^L, 0)$ , or (c) the stable manifold of  $(U^L, 0)$  lies below the unstable manifold of  $(U^R, 0)$ . In case (c), the unstable manifold of  $(U^R, 0)$  approaches the spiral sink  $(U^M, 0)$  as  $z \rightarrow \infty$ , see Figure 3c.



(a)

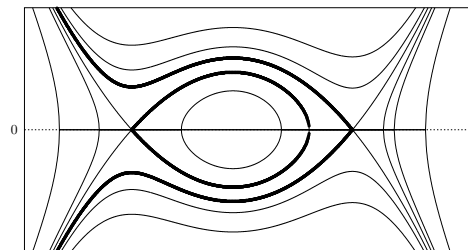


(b)

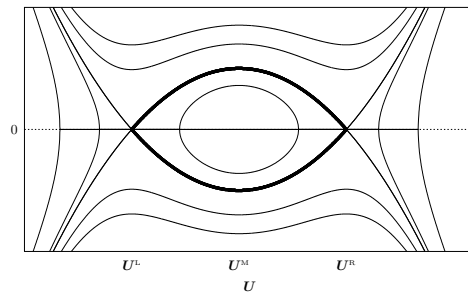


(c)

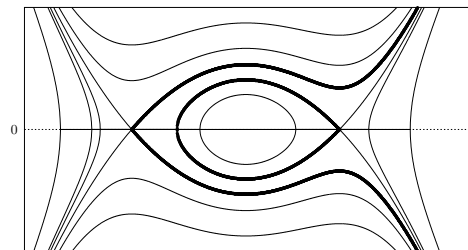
FIGURE 3. Phase plane for the nonlinear damped equation (1.1) with  $c = c(\omega)$  chosen for the existence of a heteroclinic connection (b – middle). Breaking of the saddle-saddle connection for perturbed parameters  $c \neq c(\omega)$ :  $c < c(\omega)$  (a – top),  $c > c(\omega)$  (c – bottom).



(a)



(b)



(c)

FIGURE 4. Phase plane for the nonlinear undamped equation (1.1) with parameters  $\omega = \omega_0$  chosen for the existence of a heteroclinic connection (b – middle). Breaking of the saddle-saddle connection for perturbed parameters  $\omega \neq \omega_0$ :  $\omega < \omega_0$  (a – top),  $\omega > \omega_0$  (c – bottom).

For the special case of  $c = 0$  in which there is no damping in the system, (2.2) is Hamiltonian with the conserved quantity,

$$(2.5) \quad H = \frac{1}{2}V^2 + \mathcal{V}(U).$$

In the phase plane  $(U^L, 0)$  and  $(U^R, 0)$  remain hyperbolic saddle points, while  $(U^M, 0)$  becomes a center, see Figure 4. A heteroclinic connection will exist only if the two maxima have the same value of the potential  $\mathcal{V}(U^L) = \mathcal{V}(U^R)$ . If this is the case, then from the symmetry of the phase plane system (2.2) for  $V \rightarrow -V$ , both monotone increasing and decreasing connections exist, see Figure 4b. This will occur at a value  $\omega = \omega_0$  corresponding to a root of  $c(\omega) = 0$ . For other values of  $\omega$  at  $c = 0$ , either  $(U^L, 0)$ , see Figure 4a, or  $(U^R, 0)$ , see Figure 4c, will have a homoclinic orbit, but no heteroclinic connection will exist.

In Section 7 we will review a constructive proof for the existence and uniqueness of the heteroclinic connection in terms of the transverse intersection of the stable and unstable manifolds in extended parameter space. The proof of existence will include persistence under small perturbations of the vector field, including the introduction of weakly nonautonomous, or slowly varying, coefficients resulting for the radial problem that we consider in Section 3.

**2.2. Exact solutions.** For completeness, we review some of the known exact traveling wave heteroclinic solutions of equation (1.1). Numerous studies have discovered classes of closed-form analytical solutions for polynomial nonlinearities  $F(U; \omega)$  (Dixon et al. [1991], Powell and Tabor [1992], Goriely [1995], Benguria and Depassier [1994]). Powell and Tabor [1992] describe a set of exact solutions for  $F(U; \omega)$  of the form (1.2) when  $f(U)$  has two terms with a special relation,

$$(2.6) \quad F(U; \omega) = -U(\omega - \beta U^k + (k+1)U^{2k}),$$

where  $k = 1, 2, 3, \dots$  is a positive integer and  $\beta, \omega > 0$  are parameters. In (2.6) we have factored  $F(U; \omega)$  to show that it is the product of  $U$  times a quadratic polynomial in  $U^k$ , hence the zeroes of  $F(U; \omega)$  can be obtained analytical as

$$(2.7) \quad \begin{aligned} U^L = 0, \quad U^M &= \left( \frac{\beta - \sqrt{\beta^2 - 4(k+1)\omega}}{2(k+1)} \right)^{1/k}, \\ U^R &= \left( \frac{\beta + \sqrt{\beta^2 - 4(k+1)\omega}}{2(k+1)} \right)^{1/k}. \end{aligned}$$

From these solutions it is clear that the range of  $\omega$  where  $F$  has three real roots is

$$(2.8) \quad 0 < \omega < \frac{\beta^2}{4(k+1)}.$$

For each value of  $\omega$  in this range,  $\omega_{\min} < \omega < \omega_{\max}$ , the integral curve for the heteroclinic solution of (2.3) is given by

$$(2.9) \quad V(U) \equiv \frac{dU}{dz} = U[U^k - (U^R)^k];$$

this equation can be integrated to yield the explicit heteroclinic solution,

$$(2.10) \quad U(z) = \frac{U^R}{[1 + (U^R)^k \exp \{k(U^R)^k(z - z_0)\}]^{1/k}},$$

where  $z_0$  is a constant of integration corresponding to translation invariance of the solution. Substituting ansatz (2.9) into (2.2) and balancing  $O(U)$  terms yields an explicit formula for the damping relation,  $c = c(\omega)$ ,

$$(2.11) \quad c(\omega) = U^R(\omega)^k - \frac{\omega}{U^R(\omega)^k},$$

where we have explicitly indicated the dependence of the root  $U^R$  on  $\omega$ , (2.7). The question of obtaining the wavespeed relation  $c = c(\omega)$  for the general form of the damped equation (2.2) has attracted some recent attention (Cisternas and Depassier [1996], Goriely [1995], Witelski, et al. [1998]). We will make use of this exact solution in a later section to present a closed-form solution of an example problem.

**3. Stationary axisymmetric front solutions of semilinear elliptic equations.** We now focus on obtaining radially symmetric, localized, positive, monotone decreasing front solutions of the semilinear elliptic equation (1.6). As was described in the introduction, these solutions are of great interest for many problems in applied physics, fluid dynamics, and mathematical biology. There is a large body of literature connected with the existence and uniqueness of nonnegative

solutions for this problem (Aronson and Weinberger [1978], Atkinson and Peletier [1986], Berestycki and Lions [1980], Brezis and Lieb [1984], Gidas et al. [1979], Jones [1983a] and [1983b], Kaper and Kwong [1988], Kuzin and Pohozaev [1997], McLeod and Serrin [1968] and [1987], Ni [1988], Terman [1987] and [1988]).

For the positive radially symmetric solutions that we seek, the elliptic equation (1.6) reduces to the nonlinear boundary value problem:

$$(3.1a) \quad \frac{d^2U}{dr^2} + \frac{n-1}{r} \frac{dU}{dr} + F(U; \omega) = 0, \quad 0 \leq r < \infty,$$

$$(3.1b) \quad \left. \frac{dU}{dr} \right|_{r=0} = 0, \quad U(r \rightarrow \infty) \rightarrow 0,$$

where  $F(U; \omega)$  is given by (1.2). This is a singular two-point boundary value problem for a nonautonomous nonlinear second order ordinary differential equation.

**3.1. Asymptotics of solutions of the radial boundary value problem.** In the far-field, i.e., as  $r \rightarrow \infty$ , equation (3.1a) can be linearized about  $U = 0$ :

$$(3.2) \quad \frac{d^2U}{dr^2} + \frac{n-1}{r} \frac{dU}{dr} - \omega U = 0.$$

This equation is a modified Bessel equation of order  $(n/2) - 1$  for  $\omega > 0$ . The solution is given in terms of a modified Bessel function of the second kind,  $U(r) = Cr^{1-n/2}K_{(n/2)-1}(\sqrt{\omega}r)$  (Abramowitz and Stegun [1965]). Using the asymptotics of the Bessel functions, this reduces to

$$(3.3) \quad U(r \rightarrow \infty) \sim C \sqrt{\frac{\pi}{2\sqrt{\omega}}} r^{-(n-1)/2} e^{-\sqrt{\omega}r}.$$

The value of the solution at the origin,  $U(0) \equiv U^0 > 0$ , is unknown and can be used to obtain the solution of boundary value problem (3.1) via a one-parameter shooting method (Kuzin and Pohozaev [1997], McLeod and Serrin [1987]) with  $U^0$  as the parameter. This method exploits the property of continuous dependence of solutions on initial conditions in a clear way. We now show that  $U^0$  must lie in the interval  $(U^M, U^R]$  for monotonically decreasing radial solutions to exist. The analysis

proceeds in two steps; first, we analyze the system linearized about  $U = U^0$ , then, a comparison argument is made to establish the desired result.

Near the origin, solutions of (3.1) are given by a power series expansion in  $r^2$  as  $r \rightarrow 0$ ,

$$(3.4) \quad U(r \rightarrow 0) \sim U^0 - \frac{F(U^0; \omega)}{2n} r^2 \left( 1 - \frac{F'(U^0; \omega)}{4(n+2)} r^2 + O(r^4) \right).$$

Linearizing problem (3.1) about  $U = U^0$  yields another Bessel equation, similar to (3.2), and hence the local solution can also be expressed in the form

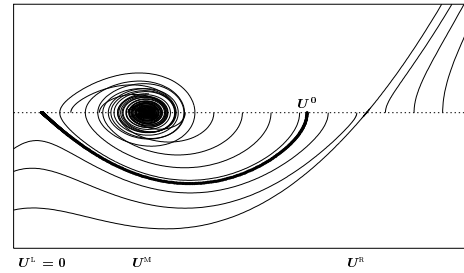
$$(3.5) \quad U(r \rightarrow 0) \sim U^0 - \frac{F(U^0; \omega)}{F'(U^0; \omega)} \cdot \left( 1 - \Gamma\left(\frac{n}{2}\right) \left(\frac{1}{2} \sqrt{|F'(U^0; \omega)|} r\right)^{1-(n/2)} \mathcal{B}_{(n/2)-1}(\sqrt{|F'(U^0; \omega)|} r) \right),$$

where  $\mathcal{B}_\nu(z)$  represents the regular or modified Bessel functions of the first kind according to

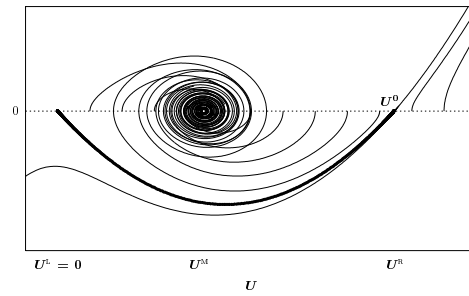
$$\mathcal{B}_\nu(z) = \begin{cases} J_\nu(z) & F'(U^0; \omega) > 0, \\ I_\nu(z) & F'(U^0; \omega) < 0. \end{cases}$$

Recall that, for all real  $\nu$ ,  $J_\nu(z)$  is a decaying oscillatory function, while  $I_\nu(z)$  is monotone increasing. When the value of  $U^0$  passes through the root of  $F'(U^0; \omega) = 0$ , the linearized behavior of the solution changes from oscillatory (Chen and Lu [1997]), suggesting the influence of the spiral sink  $U^M$ , to monotone growth, suggesting the influence of the saddle point  $U^R$ . When  $U^0$  exactly satisfies  $F'(U^0; \omega) = 0$ , the local solution degenerates to the quadratic polynomial given by (3.4).

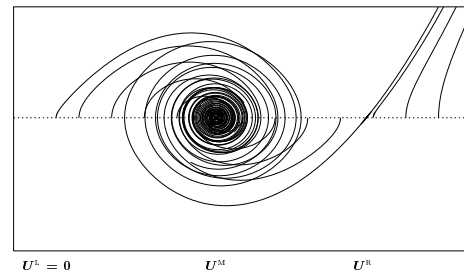
We now use the results obtained from the linearized analysis to carry out a comparison argument for the desired solution of the nonlinear problem. Solutions with  $U^0 > U^R$  are monotone increasing and can be uniformly bounded from below by the modified Bessel function solution (3.5), see Figure 5. Therefore, we conclude that, if a monotone decreasing radial solution exists, it must satisfy the condition  $U^M < U^0 \leq U^R$ , see Figure 5ab. Note from (3.4) that if  $U^0 < U^M$  then the solution is not monotone decreasing in a neighborhood of  $r = 0$ . In the



(a)



(b)



(c)

FIGURE 5. Plots of the trajectories obtained by numerically integrating the non-autonomous equation (3.1a) in the  $(U, V)$  plane. Solutions are shown for a series of uniformly spaced initial conditions chosen along the  $U$ -axis over a range of values of  $U(0) = U^0$ . The plots obtained using three distinct values of  $\omega$  are shown. If a solution of the boundary value problem (3.1) exists, it is shown as a darkened curve. In (a – top) the solution is given by the stable manifold of  $U^L$  with some  $U^0 \in (U^M, U^R)$ . In (b – middle) the solution is approximately a heteroclinic connection with  $U^0 \sim U^R$ . In (c – bottom) there is no positive localized radial solution.

limiting case that  $U^0 \rightarrow U^R$ , the solution approaches the heteroclinic connection between the saddle points at  $U^L = 0$  and  $U^R$ , see Figure 5b. When  $U^0 \ll U^R$ , we are no longer seeking a heteroclinic connection, but just the portion of the stable manifold of the point  $U^L = 0$  for  $0 \leq r < \infty$ . Finally, for values of  $\omega$  when the unstable manifold of  $U^R$  approaches the spiral sink at  $U^M$  for  $r \rightarrow \infty$ , then no positive monotone decreasing solution exists, see Figure 5c. Note the close parallels between the structure of Figure 5 and the phase plane for the autonomous problem shown in Figure 3.

**3.2. Integral formulation of the radial problem.** To gain more insight into the nature of the solution of (3.1), we rewrite (3.1a) using an integral formulation. Integrating equation (3.1a) over the entire domain with a weight function of  $r^{2(n-1)}U'(r)$ ,

$$(3.7) \quad \int_0^\infty \left[ \frac{1}{r^{n-1}} \frac{d}{dr} \left( r^{n-1} \frac{dU}{dr} \right) + F(U; \omega) \right] \frac{dU}{dr} r^{2(n-1)} dr = 0,$$

yields

$$(3.8) \quad -\frac{1}{2} \left( r^{n-1} \frac{dU}{dr} \right)^2 \Big|_0^\infty = \int_0^\infty r^{2(n-1)} F(U; \omega) \frac{dU}{dr} dr.$$

From the boundary condition (3.1b) at  $r = 0$  and the far-field asymptotics for  $r \rightarrow \infty$  (3.3), we conclude that the boundary terms on the left, and hence also the integral on the right side of this equation, vanish. Since we seek monotone decreasing solutions  $U = U(r)$ , these solutions have well-defined inverse functions  $r = r(U) \geq 0$  for  $0 \leq U \leq U^0$ . Hence, we can write the integral on the right as

$$(3.9) \quad \int_0^{U^0} F(U; \omega) r(U)^{2(n-1)} dU = I_- + I_+ = 0,$$

where

$$(3.10) \quad \begin{aligned} I_- &= \int_0^{U^M} F(U; \omega) r(U)^{2(n-1)} dU < 0, \\ I_+ &= \int_{U^M}^{U^0} F(U; \omega) r(U)^{2(n-1)} dU > 0. \end{aligned}$$

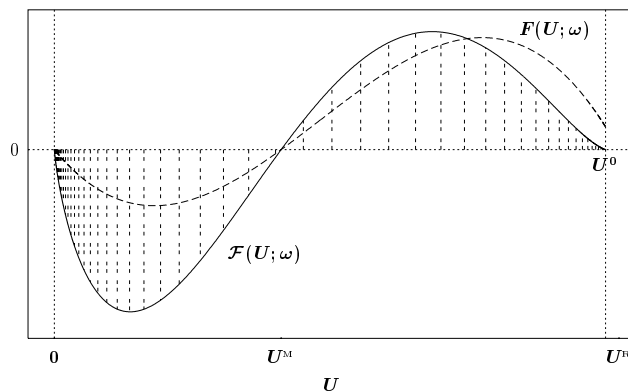


FIGURE 6. Comparison of  $F(U; \omega)$  and the equal-area rule for the weighted nonlinear function  $\mathcal{F}(U; \omega) = F(U; \omega)r(U)^{2(n-1)}$ .

Note that  $r(U)$  is positive for all  $U$ ,  $0 \leq U < U^0$ , while  $F(U; \omega)$  is negative for  $0 \leq U \leq U^M$  and positive for  $U^M < U \leq U^0$ . Consequently, equation (3.9) expresses a weighted balance between positive and negative contributions of the nonlinearity  $F(U; \omega)$ . Recall that  $F(U; \omega)$  has zeros at  $U^L = 0, U^M$ , and  $U^R$ . From the far field exponential behavior of  $U(r \rightarrow \infty) \rightarrow 0$ , (3.3), we see that  $r(U)$  must diverge logarithmically  $r(U \rightarrow 0) \rightarrow \infty$ . From the boundary condition at the origin, we see that  $r'(U \rightarrow U^0) \rightarrow -\infty$  is an integrable singularity as  $r \rightarrow 0$ . Consequently, the integrand  $\mathcal{F}(U; \omega) = F(U; \omega)r(U)^{2(n-1)}$  is a generalization of the nonlinear function  $F(U; \omega)$ , with the zeros at  $0, U^M$ , and  $U^0$ . Equation (3.9) can be interpreted as an equal-area rule for  $\mathcal{F}(U; \omega)$  (Rubinstein and Sternberg [1992], Witelski [1996], Witelski et al. [1998]), see Figure 6. For  $n = 1$ , (3.9) trivially reduces to an equal-area rule for  $F(U; \omega)$ . We will now examine under what conditions this reduction occurs for  $n > 1$ .

### 3.3. Generalized equal area rule for sharp interfaces solutions.

To understand the implications of this integral relation for the structure of monotone front solutions, we consider a special limiting case. Assume that the front connects  $U^L$  to  $U^0$ , with intermediate values,  $U \in (0, U^0)$ , being covered in a transition layer whose width is narrow compared to its radial distance from the origin. This is often called a sharp interface approximation (Caginalp [1991], Taylor and Cahn

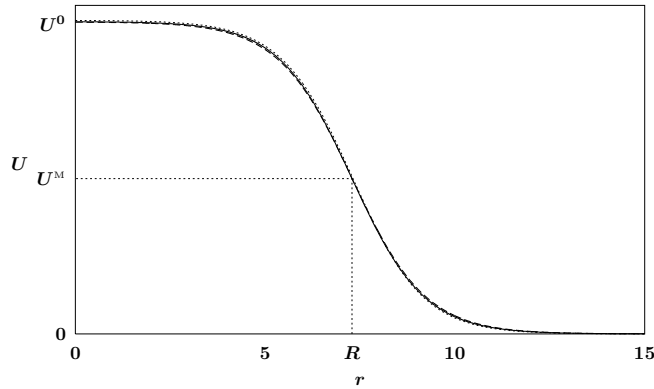


FIGURE 7. The axisymmetric sharp-interface approximate solution (4.7), (4.9), and the exact numerical solution  $U(r)$  of (3.1) showing the position of the transition front,  $r = R$ .

[1994]). Let  $r = R$  denote the position of this transition layer, and let  $\tilde{r}(U)$  be the relative displacement from  $R$ , see Figure 7,

$$(3.11) \quad r(U) = R + \tilde{r}(U).$$

A natural definition for the position of the front is the value of  $r$  where  $U = U^M$ . This choice implies  $F = 0$  at  $\tilde{r} = 0$ :

$$(3.12) \quad U^M = U(R) \iff R = r(U^M).$$

This value also marks the boundary between the positive and negative contributions to the integral relation for  $\mathcal{F}(U; \omega)$ , (3.10).

For narrow transition layers  $|\tilde{r}(U)| \ll R$  for all values of  $U$  except in small neighborhoods of  $U = U^L$  and  $U = U^0$ . Examining the integral relation (3.9), one sees that  $\mathcal{F}(U; \omega)$  vanishes in those limits, and to leading order in  $O(\tilde{r})$  one obtains

$$(3.13) \quad \int_0^{U^0} \mathcal{F}(U; \omega) dU \sim R^{2(n-1)} \int_0^{U^0} F(U; \omega) dU = 0.$$

Hence the equal area rule for  $\mathcal{F}(U; \omega)$  reduces to one for  $F(U; \omega)$ , and in this limit, the root  $U^0$  of  $\mathcal{F}(U; \omega)$  must approach the root  $U^R$  of  $F(U; \omega)$  for a particular value of  $\omega_0$  where  $F(U; \omega)$  has a heteroclinic

solution. We will see that the width of the front is inversely related to the magnitude of the eigenvalues of the two saddle points, and if we assume that those eigenvalues remain bounded, then the front will have an  $O(1)$  width. Therefore, in the limiting case of a “narrow transition layer,”  $|\tilde{r}| \ll R$  implies that the radial position of the front is going to infinity, i.e.,  $R \rightarrow \infty$ . As will be discussed further, this behavior could have been expected, since for large radii, the local curvature of the front is small, and the results known for one-dimensional planar fronts will be recovered (Tyson and Keener [1988]). In the following sections, we study how weak curvature effects have been traditionally incorporated in perturbation expansions and how leading order curvature effects can be used to obtain approximate front solutions of the radial differential equation.

#### 4.1. The autonomous approximation of the radial solution.

Motivated by the results of the previous section, we now present a heuristic construction of an approximate radial solution with a sharp interface. These localized solutions have a finite mass with exponential decay to  $U(r \rightarrow \infty) \rightarrow 0$ . In Sections 5 and 6, we will compare the accuracy of this approximate solution with a formal asymptotic expansion obtained from a regular perturbation series.

Writing the independent variable as the sum,  $r = R + \tilde{r}$ , of the position of the transition front,  $R$ , and the relative displacement from the front,  $\tilde{r}$ , we put (3.1a) in the form

$$(4.1) \quad \frac{d^2U}{d\tilde{r}^2} + \frac{n-1}{R+\tilde{r}} \frac{dU}{d\tilde{r}} + F(U; \omega) = 0.$$

If the front is a sharp transition layer occurring at a large distance from the origin, large relative to the width of the front,  $R \gg \tilde{r}$ , then the coefficient of the damping term can be expanded as

$$(4.2) \quad \frac{n-1}{R+\tilde{r}} = c - \frac{(n-1)\tilde{r}}{R^2} + \frac{(n-1)\tilde{r}^2}{R^3} + O(R^{-4}), \quad c = \frac{n-1}{R},$$

for  $R \rightarrow \infty$ . Retaining the leading order term from this expansion reduces (4.1) to

$$(4.3) \quad \frac{d^2\tilde{U}}{d\tilde{r}^2} + c \frac{d\tilde{U}}{d\tilde{r}} + F(\tilde{U}; \omega) = 0.$$

This is just the autonomous damped equation of the form (1.1) that was solved in Section 2 to yield bounded heteroclinic connections for all  $\omega \in (\omega_{\min}, \omega_{\max})$  and  $c = c(\omega)$ .

Solutions of (4.3) are translation invariant under  $\tilde{r} \rightarrow \tilde{r} + \tilde{r}_0$ , leaving the position of the front unspecified. However, using (3.12) as the definition of the front position,  $R$ , we can select a unique solution from the continuous one-parameter translation invariant family. We now present an example of this approximation that yields a closed-form radial solution.

**4.1. An example.** Consider the problem of finding the unique localized solution of the radial differential equation

$$(4.4) \quad \frac{d^2U}{dr^2} + \frac{n-1}{r} \frac{dU}{dr} - \omega U + 3U^2 - 2U^3 = 0.$$

This problem is analogous to the nonlinear eigenvalue problem for spherical polymer globules solved in (Witelski et al. [1998]) with  $n = 3$  and  $\omega > 0$ . Using the large-radius approximation described above, we write the corresponding autonomous equation (4.3) as

$$(4.5) \quad \frac{d^2\tilde{U}}{d\tilde{r}^2} + c \frac{d\tilde{U}}{d\tilde{r}} - \omega \tilde{U} + 3\tilde{U}^2 - 2\tilde{U}^3 = 0.$$

We recognize (4.5) as an exactly solvable problem of the form (2.6) with  $k = 1$ ,  $\beta = 3$ , and use the results obtained in Section 2.2. The equilibrium solutions of (4.4) and (4.5) are

$$(4.6) \quad U^L = 0, \quad U^M = \frac{3 - \sqrt{9 - 8\omega}}{4}, \quad U^R = \frac{3 + \sqrt{9 - 8\omega}}{4},$$

for the range  $0 \leq \omega < 9/8$ . The explicit heteroclinic solution of (4.5) is

$$(4.7) \quad \tilde{U}(\tilde{r}) = \frac{U^R U^M}{U^M + (U^R - U^M) \exp[U^R \tilde{r}]},$$

where the phase condition  $\tilde{U}(\tilde{r} = 0) = U^M$ , (3.12), has been satisfied. The relation for  $c(\omega)$  may now be obtained by plugging  $U^R$  into (2.11):

$$(4.8) \quad c(\omega) = \frac{6(1 - \omega)}{1 + \sqrt{9 - 8\omega}}.$$

Finally, substituting (4.8) into (4.2) yields an approximation for the core radius,  $\tilde{R}$ :

$$(4.9) \quad \tilde{R} = (n-1) \frac{1 + \sqrt{9 - 8\omega}}{6(1 - \omega)}.$$

Combining (4.7) and (4.9) gives us the approximate solution of (4.4) as  $U(r) \approx \tilde{U}(r - \tilde{R})$ . A search of the scientific literature reveals that this approximation has been used in an ad hoc manner earlier in chemical physics (Chan [1977]), among other places. In later subsections, we analyze the limits of validity of this solution in comparison with an asymptotic expansion of the solution of the full problem.

**4.2. Properties of the localized solution.** Before carrying out this comparison, it is useful to describe the properties of the solution that are of primary interest in applications. We tie this description to the problem of finding the structure of the collapsed polymer globule state from Witelski et al. [1998], though it is equally relevant to all of the other problems described in the introduction. Our primary focus has been the structure of the sharp interface, or transition layer, forming the boundary between the high density inner core of the solution, where  $U \approx U^0 \approx U^R$ , and the surrounding empty space,  $U = 0$ , see Figures 1, 7. There are well-developed experimental and theoretical works giving a variety of results for problems with these phase transition interfaces, see for example Bates and Fife [1993], Lifschitz and Freed [1993], Pego [1989], Puri and Binder [1991], Witelski [1998]). First, we observe that, by (4.7), the dimensionality of the solution,  $n = 1$  for planar interfaces,  $n = 2$  cylindrical, or  $n = 3$  spherical solutions, does not affect the local density profile structure of the interface. Instead, the dimensionality enters through the core radius  $\tilde{R}$  (4.9). Second, equation (4.5) supports heteroclinic solutions for a range of  $\omega$ , corresponding to a range of system temperatures or levels of kinetic energy, namely  $0 \leq \omega < 9/8$ . However, for equation (4.9) to describe a physically meaningful finite positive core radius, only a reduced range of  $\omega$ , namely  $0 \leq \omega < 1$ , can be used. In the limit  $\omega \rightarrow 1$ , we approach the infinite radius solution  $\tilde{R} \rightarrow \infty$ . Since the curvature is inversely proportional to  $\tilde{R}$ , this limit returns the planar front solution. Note that excellent agreement with the exact solution is achieved even for moderate radii, as shown in Figure 7 for  $n = 2$ ,  $\omega = 0.95$  and  $R \approx 7.22$ . Finally, for the range

$1 < \omega < 9/8$ , no localized positive radial solutions of (4.4) are expected to exist.

For the many problems in which the transition is narrow compared to the radius of the inner core, the sharp interface approximation is useful, and one can directly compute the mass, or integral, of the radially symmetric solution:

$$(4.10) \quad M = \frac{2\pi^{n/2}}{\Gamma(n/2)} \int_0^\infty U(r)r^{n-1} dr.$$

To leading order, in the sharp interface approximation, we can replace the smoothed exponential solution (4.7) by a limiting step function:

$$(4.11) \quad U(r) \approx \tilde{U}(-\tilde{R})H(\tilde{R} - r),$$

where  $H(z)$  is the Heaviside step function, and  $U^0 \approx \tilde{U}(-\tilde{R})$  is used as an approximation of the uniform core density. This yields the following closed-form estimate of the mass:

$$(4.12) \quad M = \frac{2\pi^{n/2}\tilde{R}^n}{n\Gamma(n/2)}\tilde{U}(-\tilde{R}).$$

We now turn to compare this solution with asymptotic expansions for the solution of (4.1).

**5. Asymptotic analysis of the radial problem.** In this section we present a regular perturbation series solution to the radial problem (3.1). The solution is expanded about a stationary planar interface solution, and it incorporates curvature of the front in higher order corrections.

Using the same change of variables employed in Section 4, namely  $r = R + \tilde{r}$ , we start with (4.1):

$$(5.1) \quad \frac{d^2U}{d\tilde{r}^2} + \frac{n-1}{R+\tilde{r}} \frac{dU}{d\tilde{r}} + F(U; \omega) = 0.$$

The primary weaknesses of the approximate solution given in Section 4 are the lack of information about the limits of its validity and the absence of a clear method for estimating the error and improving the

approximation. These problems can be corrected with a more careful justification of the expansion of the damping coefficient (4.2). Formula (4.2) is an asymptotic expansion in the limit  $R \rightarrow \infty$ . From the integral formulation of problem (3.1) presented in Sections 3.2 and 3.3, we recognize that this limit occurs only for a special value of  $\omega$ ,  $\omega = \omega_0$ , where  $F(U; \omega_0)$  satisfies the equal area rule,

$$(5.2) \quad \int_{U^L(\omega_0)}^{U^R(\omega_0)} F(U; \omega_0) dU = 0.$$

Hence we will write  $\omega = \omega_0 - \varepsilon$ , where  $0 \leq \varepsilon \ll 1$  is a detuning parameter (Kevorkian and Cole [1996]) that will serve as the basis of our perturbation expansion. The problem we solve can then be written as

$$(5.3a) \quad \frac{d^2 U}{d\tilde{r}^2} + \frac{n-1}{R+\tilde{r}} \frac{dU}{d\tilde{r}} + F(U; \omega_0 - \varepsilon) = 0, \quad -\infty < \tilde{r} < \infty,$$

with boundary conditions (3.1b) for  $|\tilde{r}| \rightarrow \infty$  and the phase condition (3.12):

$$(5.3b) \quad U'(\tilde{r} \rightarrow -\infty) \rightarrow 0, \quad U(\tilde{r} \rightarrow \infty) \rightarrow 0, \quad U(\tilde{r} = 0) = U^M.$$

**5.1. Regular perturbation expansions.** Our solution will be given as a regular perturbation expansion for  $U(\tilde{r})$ ,

$$(5.4a) \quad U(\tilde{r}) = U_0(\tilde{r}) + \varepsilon U_1(\tilde{r}) + \varepsilon^2 U_2(\tilde{r}) + \dots,$$

along with a strained parameter expansion for the position of the front:

$$(5.4b) \quad R = \frac{1}{\varepsilon} R_{-1} + R_0 + \varepsilon R_1 + \varepsilon^2 R_2 + \dots$$

Moreover, since  $U^M = U^M(\omega)$ , (2.7), we expand the phase condition as:

$$(5.5) \quad U^M = U_0^M + \varepsilon U_1^M + \varepsilon^2 U_2^M + \dots$$

To leading order, we obtain a nonlinear autonomous equation for  $U_0(\tilde{r})$ :

$$(5.6) \quad \mathcal{N}[U_0] \equiv \frac{d^2 U_0}{d\tilde{r}^2} + F(U_0; \omega_0) = 0.$$

This equation is an undamped Hamiltonian equation that possesses a unique monotone decreasing heteroclinic solution satisfying the condition  $U_0(0) = U_0^M$ . Its solution describes a stationary one-dimensional planar front, and it does not include any curvature effects or determine any finite radius contributions to the speed of the front. A representation for its integral curve may be found implicitly in terms of  $V = V_0(U)$  as follows. Since  $V_0(U) = dU_0/d\tilde{r}$ , a straight-forward calculation gives  $U_0''(\tilde{r}) = dV_0/d\tilde{r} = V_0(U)V_0'(U)$  (Bender and Orszag [1978]). Hence, equation (5.5) is transformed into the first order differential equation

$$(5.6) \quad V_0 \frac{dV_0}{dU} + F(U; \omega_0) = 0.$$

Direct integration then yields the integral curve  $V_0(U)$  for the heteroclinic orbit,

$$(5.7) \quad V_0(U) = -\sqrt{\omega_0 U^2 - 2 \int_0^U f(u) du}.$$

At higher orders, the expansions yield inhomogeneous linear problems for  $U_k(\tilde{r})$ ,  $k = 1, 2, 3, \dots$ ,

$$(5.8a) \quad \mathcal{L}U_1 = \mathcal{R}_1(U_0, R_{-1}) \equiv -U_0 - \frac{n-1}{R_{-1}} \frac{dU_0}{d\tilde{r}},$$

$$(5.8b) \quad \begin{aligned} \mathcal{L}U_2 &= \mathcal{R}_2(\tilde{r}, U_0, U_1, R_{-1}, R_0) \\ &\equiv -U_1 - \frac{1}{2}f''(U_0)U_1^2 - \frac{n-1}{R_{-1}} \frac{dU_1}{d\tilde{r}} + \frac{(n-1)(R_0 + \tilde{r})}{(R_{-1})^2} \frac{dU_0}{d\tilde{r}}, \end{aligned}$$

$$(5.8c) \quad \mathcal{L}U_k = \mathcal{R}_k(\tilde{r}, \dots, U_{k-1}, \dots, R_{k-2}), \quad k = 2, 3, \dots$$

Here, the linear operator is the functional derivative of  $\mathcal{N}$ , which is given by (5.5),

$$(5.9) \quad \mathcal{L}U \equiv \left( \frac{\delta \mathcal{N}}{\delta U} \Big|_{U_0} \right) U = \frac{d^2 U}{d\tilde{r}^2} + [f'(U_0) - \omega_0]U.$$

To solve for the functions  $U_1, U_2, \dots$  in (5.4a), we need to consider the properties of the linear operator  $\mathcal{L}$  given by (5.9). If any of the terms in (5.4a) are not bounded for all  $\tilde{r}$ , then the expansion may not be uniformly well-ordered in an asymptotic sense. To suppress terms that would yield unbounded growth in  $U_k(\tilde{r})$  as  $|\tilde{r}| \rightarrow \infty$ , we apply the Fredholm alternative (Friedman [1990]) to obtain a solvability condition at each order in the expansion:

$$(5.10) \quad \int_{-\infty}^{\infty} \mathcal{R}_k(\tilde{r}, \dots, R_{k-2})W(\tilde{r}) d\tilde{r} = 0,$$

where  $W(\tilde{r})$  is an element of the null space of the adjoint operator. This function  $W(\tilde{r})$  is a solution of the problem

$$(5.11) \quad \mathcal{L}^\dagger W = 0, \quad W'(\tilde{r} \rightarrow -\infty) \rightarrow 0, \quad W(\tilde{r} \rightarrow \infty) \rightarrow 0.$$

Since the operator is self-adjoint (Friedman [1990]),  $\mathcal{L}^\dagger = \mathcal{L}$ , the adjoint solution is  $W(\tilde{r}) = U'_0(\tilde{r})$ . Consequently, at each order, i.e., for each  $k = 1, 2, \dots$ , equation (5.10) yields a solvability condition in terms of the lower order solutions  $U_0, \dots, U_{k-1}$  and  $R_{-1}, \dots, R_{k-3}$  that uniquely determines the value of the next correction to the front position  $R_{k-2}$  so that secular growth is eliminated from the solution  $U_k(\tilde{r})$ .

To calculate the leading order term,  $R_{-1}$ , in the expansion of the front position, (5.4b), it suffices to evaluate the function  $\mathcal{R}_1$  for the function  $U'_0(\tilde{r}) = V_0(U)$  given by (5.7), and then to substitute the result into the solvability condition (5.10) with  $k = 1$ . Integrating the first term, observing that only the lower limit of integration yields a nonzero contribution, and transforming the variable of integration in the second term from  $\tilde{r}$  to  $U$ , we arrive at:

$$(5.12) \quad R_{-1} = -\frac{2(n-1)}{U^R(\omega_0)^2} \int_0^{U^R(\omega_0)} V_0(U) dU > 0,$$

see also Witelski et al. [1998].

**5.2. An example.** To illustrate the solution procedure discussed in Section 5.1, we return to the example given by equation (4.4), with  $F(U; \omega) = -2U^3 + 3U^2 - \omega U$  and  $n = 2$ . The equal-area condition

(5.2) is satisfied for  $\omega_0 = 1$  on the interval  $(U^L = 0) \leq U \leq (U^R = 1)$ . Therefore, we write  $\omega = 1 - \varepsilon$ . Using the perturbation expansions given above, we obtain the solution,  $U \sim U_\varepsilon(\tilde{r})$ :

$$(5.13) \quad U_\varepsilon(\tilde{r}) = \frac{1}{1 + e^{\tilde{r}}} + \varepsilon \frac{(5 + \tilde{r})e^{\tilde{r}} - 1}{(1 + e^{\tilde{r}})^2} + O(\varepsilon^2),$$

and the corresponding front position is given by

$$(5.14) \quad R = \frac{1}{3\varepsilon} + \frac{2}{3} + \frac{14}{3}\varepsilon + O(\varepsilon^2).$$

The structure of the solution  $U(r) \sim U_\varepsilon(r - R)$  matches the numerically-obtained exact solutions very well for all moderate and large values of  $R$ , as shown in Figure 7. However, for small  $R$ , i.e., for the case of solutions for which the front position is very close to the origin, the expansion becomes much less accurate.

From Figure 8, we see that the expansion of the front position (5.14) approximates the exact front position, as calculated from a direct numerical solution of (4.4), quite well. Moreover, it is asymptotically accurate as  $\varepsilon \rightarrow 0$ , i.e., as  $\omega \rightarrow 1$ . In fact, the expansion carried out to  $O(\varepsilon^2)$  has a wider range of validity than the expression for the approximate front position  $\tilde{R}$ , given by (4.9), in Section 4.1. In the next subsection, we will make precise the relation of the approximate solution (4.7), (4.9) to the asymptotic solution (5.13), (5.14) and discuss the advantages of the approximate solution over the asymptotic expansion given above.

We note that the  $O(\varepsilon^2)$  term in the expansion of  $U_\varepsilon(\tilde{r})$ ,  $U_2(\tilde{r})$ , is given by a cumbersome expression, involving the dilogarithm special function (Lewin [1981]),

$$(5.15) \quad \text{Li}_2(z) = - \int_0^z \frac{\ln(1 - s)}{s} ds,$$

which arises from integrals of the inhomogeneous terms in equation (5.8b). Higher order terms in the expansion will contain more complicated polylogarithms, which are generalizations of (5.15).

**5.3. Analysis of the autonomous approximate solution (4.7).**

In order to compare the approximate solution, (4.7) and (4.9), found in

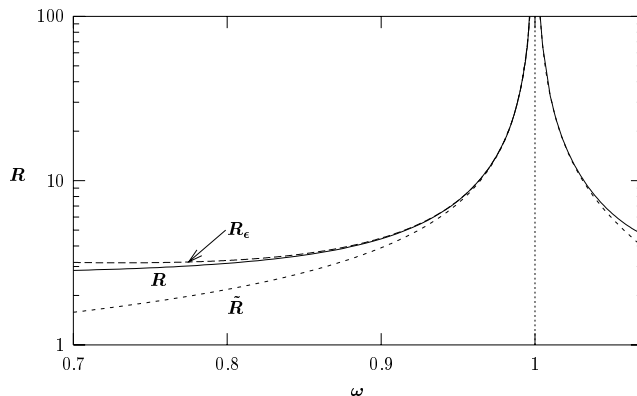


FIGURE 8. Comparison of the numerically obtained exact front position, or core radius,  $R$ , for problem (4.4), with the results of the asymptotic expansion,  $R_\epsilon$  from (5.14), and the approximate front position,  $\tilde{R}$  from (4.9) for a range of different values of the parameter  $\omega$ . See Section 8 for a discussion of  $\omega > \omega_0 = 1$ .

Section 4.1 with the asymptotic expansion determined above, we write  $\omega$  as  $\omega = 1 - \varepsilon$  in equations (4.6), (4.7) and (4.9). Then, by expanding (4.7) in the limit  $\varepsilon \rightarrow 0$ , we obtain:

(5.16)

$$\begin{aligned} \tilde{U}(\tilde{r}) = & \frac{1}{1 + e^{\tilde{r}}} + \varepsilon \frac{(5 + \tilde{r})e^{\tilde{r}} - 1}{(1 + e^{\tilde{r}})^2} \\ & + \varepsilon^2 \frac{(\tilde{r}^2 + 14\tilde{r} + 56)e^{2\tilde{r}} - (\tilde{r}^2 + 10\tilde{r} + 20)e^{\tilde{r}} - 4}{2(1 + e^{\tilde{r}})^3} + O(\varepsilon^3), \end{aligned}$$

and the front position (4.9) is approximated by:

$$(5.17) \quad \tilde{R} = \frac{1}{3\varepsilon} + \frac{2}{3} - \frac{4}{3}\varepsilon + O(\varepsilon^2).$$

The first two terms in the expansion for  $\tilde{U}(\tilde{r})$  in (5.16) exactly match those for  $U_\varepsilon(\tilde{r})$  found above in (5.13), and similarly for the first two terms in the respective expansions for  $R$  and  $\tilde{R}$ . However, the second order correction terms differ. The  $O(\varepsilon^2)$  term in (5.16) is a rational polynomial function of  $\tilde{r}$  and  $e^{\tilde{r}}$ , and it does not contain the dilogarithm terms (5.15) found in  $U_2(\tilde{r})$ , as was described above. Also,  $\tilde{R}_1 = -4/3$  in equation (5.17) does not match the correct asymptotic coefficient

$R_1 = 14/3$  that was found above in (5.14). Therefore, in this example we have seen that the approximate solution (5.16) captures both the correct leading order solution and the first order correction terms in the asymptotic expansion of the interface structure and the radial front position. In the next subsection, we demonstrate that this is true for the problem for equation (5.1) with general bi-stable  $F(U; \omega)$  as well.

**5.4. Analysis of the general autonomous approximate solution.** As a preliminary step, we make some general observations about the nature of the large front-radius limit,  $R \rightarrow \infty$ . Recall from Section 3 that the linearized behavior of the radial solution for  $r \rightarrow \infty$  is  $U \sim Cr^{-(n-1)/2}e^{-\sqrt{\omega}r}$ , (3.3). In contrast, the asymptotic behavior of the heteroclinic solution is  $\tilde{U} \sim \tilde{C}e^{\lambda_-^L \tilde{r}}$ , where the exponential decay rate is given by the eigenvalue (2.4), with  $U^E = U^L$ . Using  $f'(U^L) = 0$  from (1.2) and  $c \sim (n-1)/(R + \tilde{r})$  from (4.2), we get the following expansion:

$$(5.18) \quad \lambda_-^L = -\sqrt{\omega} - \frac{n-1}{2(R + \tilde{r})} + O(R^{-2}),$$

as  $R \rightarrow \infty$ . Note that the leading term of (5.18) gives the correct rate of exponential decay matching (3.3), sometimes called the controlling factor (Bender and Orszag [1978]). Furthermore, if  $\lambda_-^L$  is interpreted as the derivative of the phase,  $\lambda_-^L = S'(\tilde{r})$ , in a WKB approximation (Bender and Orszag [1978]) of  $\tilde{U}(\tilde{r}) \sim e^{S(\tilde{r})}$  as  $\tilde{r} \rightarrow \infty$ , then we recover the full leading order behavior,

$$(5.19) \quad \tilde{U}(\tilde{r} \rightarrow \infty) \sim \tilde{C}(R + \tilde{r})^{-(n-1)/2}e^{-\sqrt{\omega}\tilde{r}}.$$

Hence, the approximate solution is consistent with the far-field asymptotics of the exact solution.

We now establish the limitations on the order of accuracy of the approximate solution constructed in Section 4 by comparing it to the asymptotic expansion of the exact solution, constructed in Section 5.1. By comparing the terms in the respective series expansions for  $\varepsilon \rightarrow 0$  we will show that the first discrepancies occur at  $O(\varepsilon^2)$  for  $U(\tilde{r})$  and at  $O(\varepsilon)$  for  $R$ . Recall that the approximation made in reducing the nonautonomous equation (4.1) to the damped autonomous equation (4.3) was in retaining only the leading term in the geometric series

expansion for the non-autonomous damping coefficient as  $R \rightarrow \infty$ , (4.2). The full series is given by (4.2). Consequently, the first correction term is

$$(5.20) \quad -\frac{(n-1)\tilde{r}}{R^2} \frac{d\tilde{U}}{d\tilde{r}} \sim -\frac{(n-1)\tilde{r}}{(R_{-1})^2} \frac{dU_0}{d\tilde{r}} \varepsilon^2 = O(\varepsilon^2).$$

This is the first explicitly nonautonomous term that occurs in the perturbation expansion of equation (5.3a), and it comes in at  $O(\varepsilon^2)$  in equation (5.8b). This term is uniformly bounded by  $O(\varepsilon^2)$  as  $\varepsilon \rightarrow 0$  for the heteroclinic solution, and it is exponentially small outside of a neighborhood of the front at  $\tilde{r} = 0$ , since  $dU_0/d\tilde{r}$  decays exponentially for large  $\tilde{r}$ . While the nonautonomous coefficient in this term grows algebraically away from the front, the derivative of the leading order solution decays exponentially.

To see the effect of this term in the perturbation expansion, we need to distinguish autonomous terms from explicitly  $\tilde{r}$ -dependent inhomogeneous terms in (5.8). Consider rewriting the asymptotic expansions (5.4) in terms of the autonomous approximate solution and an expansion of the correction to that approximation:

$$(5.21) \quad U(\tilde{r}) = \tilde{U}(\tilde{r}, \varepsilon) + \hat{U}(\tilde{r}, \varepsilon), \quad \hat{U}(\tilde{r}, \varepsilon) = \sum_{k=0}^{\infty} \varepsilon^k \hat{U}_k(\tilde{r}),$$

and

$$(5.22) \quad R = \tilde{R}(\varepsilon) + \hat{R}, \quad \hat{R} = \sum_{k=-1}^{\infty} \varepsilon^k \hat{R}_k.$$

Using this ansatz in equation (5.3a) and neglecting nonautonomous contributions to the damping coefficient, to leading order equation we get (4.3). We could expand this equation as a series of regular perturbation problems for  $\varepsilon \rightarrow 0$  for the autonomous equation:

$$(5.23) \quad \mathcal{N}[\tilde{U}_0] = 0,$$

and

$$\mathcal{L}\tilde{U}_k = \tilde{\mathcal{R}}_k(\dots, \tilde{U}_{k-1}, \dots, \tilde{R}_{k-2}), \quad k = 1, 2, 3, \dots,$$

where  $\tilde{\mathcal{R}}_k$  involves only autonomous terms, with no explicit dependence on  $\tilde{r}$ . However, we know that  $\tilde{U}(\tilde{r}, \varepsilon)$  is an exact solution of the autonomous equation (4.3) for all values of  $\varepsilon$  in the acceptable range of  $\omega$ . Hence, we do not need any correction to the approximate solution until non-autonomous terms enter the expansion (5.8). The autonomous problem (5.23) exactly matches (5.5) and (5.8a), therefore the autonomous approximate solution correctly reproduces  $U_0(\tilde{r})$ ,  $U_1(\tilde{r})$  and  $R_{-1}$ , and therefore  $\hat{U}_0 = \hat{U}_1 = \hat{R}_{-1} = 0$ .

At  $O(\varepsilon^2)$  the nonautonomous term (5.20) enters in equation (5.8b),

$$\begin{aligned} \mathcal{L}\tilde{U}_2 + \mathcal{L}\hat{U}_2 &= \tilde{\mathcal{R}}_2(\tilde{U}_0, \tilde{U}_1, \tilde{R}_{-1}, \tilde{R}_0) + \hat{\mathcal{R}}_2(\tilde{r}, \dots), \\ \hat{\mathcal{R}}_2 &= \frac{(n-1)\tilde{r}}{(R_{-1})^2} \frac{dU_0}{d\tilde{r}}, \end{aligned}$$

where  $\mathcal{L}\tilde{U}_2 = \tilde{\mathcal{R}}_2$ . Here, since  $\hat{\mathcal{R}}_2$  is present, we get a nonautonomous correction  $\hat{U}_2(\tilde{r})$  and therefore  $U_2(\tilde{r}) \neq \tilde{U}_2(\tilde{r})$  as observed above. At this order, the  $R_0$  coefficient in the expansion of the front position is calculated from the solvability condition (5.10) for  $\mathcal{R}_2 = \tilde{\mathcal{R}}_2 + \hat{\mathcal{R}}_2$ . We now determine the condition needed so that the nonautonomous term  $\hat{\mathcal{R}}_2$  does not yield a correction to the autonomous front coefficient  $\tilde{R}_0$ . Since  $W(\tilde{r}) = U'_0(\tilde{r})$ , the integral for the nonautonomous contribution becomes

$$(5.25) \quad \int \hat{\mathcal{R}}_2 W d\tilde{r} = \int_{-\infty}^{\infty} \tilde{r} \left( \frac{dU_0}{d\tilde{r}} \right)^2 d\tilde{r}.$$

If this term vanishes, then the autonomous solvability condition,  $\int \tilde{\mathcal{R}}_2 W d\tilde{r} = 0$ , is equivalent to the full solvability condition (5.10), and we find that  $R_0 = \tilde{R}_0$  and  $\hat{R}_0 = 0$ . We observed this behavior in the example above. However, the integral (5.25) does not generically vanish for all  $F(U; \omega)$ . It will disappear trivially if  $U'_0(\tilde{r})$  is an even function. From the implicit form of the solution  $U_0(\tilde{r})$ ,

$$(5.26) \quad \tilde{r}(U) = \int_U^{U_0^M} \frac{du}{\sqrt{-2\mathcal{V}(u)}},$$

it can be shown that  $\mathcal{V}(U)$  must be even with respect to  $U = U_0^M$  for the autonomous solvability condition to hold, where  $\mathcal{V}(U)$  is negative

over the entire interval of integration,  $U_0^L < U < U_0^R$ , see Figure 2b. For the exact solutions given in Section 2.1, we observe that  $F(U; \omega_0)$ , (2.7), is odd with respect to  $U^M$  for  $\omega_0 = 2\beta^2/(9[k+1])$ , and hence the corresponding potential  $\mathcal{V}(U)$  is symmetric. Satisfying the autonomous front condition (5.25) is yet another special and very useful property of these solutions. For problems with nonsymmetric potential functions  $\mathcal{V}(U)$ , it is still possible to obtain second order accuracy for the front position, but the definition of the front position (3.12) must be replaced by the less convenient, non-local integral condition (5.25).

The autonomous approximate solution of equation (5.1) provides an asymptotic solution in a more compact form and involving fewer calculations than the corresponding result from the regular perturbation expansion. Our construction using the solution of the single autonomous equation (4.3) eliminates the need to solve equations (5.5) and (5.8a) and the solvability integral conditions for  $R_{-1}$  and  $R_0$ . Furthermore, extending the accuracy of the approximate solution is exactly equivalent to solving for the higher order asymptotic corrections in the regular perturbation expansion. Consequently, it is clear that the autonomous approximate solution is advantageous since it provides a very convenient form of a second order accurate solution of (5.1).

**6. Instability of the equilibrium solution.** We now apply our results to provide an elementary demonstration of the fact that the localized radial solution of the elliptic equation  $\nabla^2 u + F(u; \omega) = 0$  is an unstable equilibrium of the reaction-diffusion equation

$$(6.1) \quad \frac{\partial u}{\partial t} = \nabla^2 u + F(u; \omega),$$

in  $\mathbf{R}^n$ . If  $F(u; \omega)$  is a bi-stable nonlinearity then it is well known that the solution will develop well-defined fronts connecting smooth, slowly varying outer regions (Fife [1988], Rubinstein, et al. [1989]). Suppose that we search for axisymmetric traveling wave front solutions of (6.1) of the form  $u(r, t) = U(r - \tilde{c}t)$  where  $\tilde{c}$  is the wavespeed. These solutions satisfy the differential equation

$$(6.2) \quad \frac{d^2 U}{dz^2} + \left( \tilde{c} + \frac{n-1}{r} \right) \frac{dU}{dz} + F(U; \omega) = 0,$$

where the traveling wave phase variable is  $z = r - \tilde{c}t$ . Equation (6.2) shows that, for  $\tilde{c} \neq 0$ , equation (6.1) is not separable in terms of the

variables  $z$  and  $t$  for the steady-profile traveling wave ansatz  $u = U(z)$  and hence such traveling waves are not exact solutions. More properly, the solution should be expressed in terms of a multi-scale expansion (Kevorkian and Cole [1996]) to allow the solution to slowly change shape as it evolves in  $r$  and  $t$ . However, we will show that in the large radius limit, these traveling waves give very accurate information about the behavior of problem (6.1). In fact, a multi-scale perturbation expansion of the full solution would return  $U(r - \tilde{c}t)$  as the leading order term.

We begin by expressing (6.2) as an ordinary differential equation in terms of the phase variable  $z$  alone. Note that the variable  $r$  appearing in the coefficient of the first derivative above can be written as  $r = z + \tilde{c}t$ . As was done for the equilibrium problem in (3.11), we can write the phase  $z$  in terms of the phase  $Z$  corresponding to the motion of the front and the relative displacement,  $\tilde{z}$ , from the front:

$$(6.3) \quad z = Z + \tilde{z}, \quad Z = R - \tilde{c}t,$$

where  $R = R(t)$  is the time-dependent radial position of the front. As in (3.12), we define the position of the front by the  $U^M$  level set,

$$(6.4) \quad u(R(t), t) = U^M.$$

Combining the changes of variables (6.3), we express  $r$  as

$$(6.5) \quad r = z + \tilde{c}t = R + \tilde{z},$$

reducing (6.2) to

$$(6.6) \quad \frac{d^2U}{d\tilde{z}^2} + \left( \tilde{c} + \frac{n-1}{R + \tilde{z}} \right) \frac{dU}{d\tilde{z}} + F(U; \omega) = 0.$$

We treat the factor of  $R$  appearing in (6.6) as if it were a large constant; we will justify this approximation a posteriori by showing that it is in fact a slowly varying function of time, see Kevorkian and Cole [1996] for general theory underlying this type of quasistationary approximation. Having reduced the problem to a nonautonomous differential equation in  $\tilde{z}$ , we now use an expansion of the damping coefficient for large front radius,  $R \rightarrow \infty$ ,

$$(6.7) \quad \tilde{c} + \frac{n-1}{R + \tilde{z}} = c - \frac{(n-1)\tilde{z}}{R^2} + \frac{(n-1)\tilde{z}^2}{R^3} + O(R^{-4}),$$

where

$$c = \left( \tilde{c} + \frac{n-1}{R} \right),$$

to obtain the autonomous approximation for the equation of the front structure,

$$(6.8) \quad \frac{d^2U}{d\tilde{z}^2} + c \frac{dU}{d\tilde{z}} + F(U; \omega) = 0.$$

Since (6.8) is of the form (1.1), in order to obtain a bounded monotone decreasing front solution, the damping coefficient must be determined by the relation  $c = c(\omega)$ . Hence the damping coefficient  $c$  is a time-independent constant value determined by the form of the nonlinearity  $F$  and we have a fixed relation between the front position and the wave speed,

$$(6.9) \quad \tilde{c} = c(\omega) - \frac{n-1}{R}.$$

Identifying the wavespeed  $\tilde{c}$  as the speed of the front, we see that  $\tilde{c} = dR/dt$ , and that (6.9) is a differential equation for the motion of the front,

$$(6.10) \quad \frac{dR}{dt} = c(\omega) - \frac{n-1}{R}.$$

Note that while  $R$  is large i.e., the front is bounded away well from the origin, the front speed is finite, and  $R(t)$  is slowly varying. This justifies our earlier approximation of  $R$  as a slowly varying parameter in the large radius regime.

Equation (6.10) has an equilibrium solution with radius  $\bar{R} = (n-1)/c(\omega)$ . This value is the front radius (4.9) in the solution of the equilibrium elliptic problem (4.1) since from (6.9) we have  $\tilde{c} = 0$ . This radius is called the critical nucleation radius in the context of chemical reactions and nucleation theory (Borgis and Moreau [1988], Chan [1977]). It is an unstable equilibrium that separates solutions that grow outward indefinitely from those that collapse inward toward the origin. If we have a solution with a front radius larger than the equilibrium value,  $R > \bar{R}$ , then from (6.10) we obtain a positive wavespeed  $\tilde{c} = dR/dt > 0$ . This means that the solution grows in

size as the front moves outward. Conversely, if we start with a solution with a core radius that is smaller than the equilibrium value,  $R < \bar{R}$ , then we get a negative wavespeed,  $\tilde{c} = dR/dt < 0$ . This situation describes a front moving inward toward the origin and a solution that is “collapsing.” Consequently, we conclude that the equilibrium solution is unstable to perturbations that either diminish or increase its size. In fact, we can obtain the general solution of (6.10) in implicit form,

$$(6.11) \quad t(R) = t_0 + \frac{1}{c} \left( R + \frac{n-1}{c} \ln |cR - (n-1)| \right).$$

Solution (6.11) is specified up to a time-shift constant  $t_0$ , which is determined by the initial data. In Figure 9 we compare direct numerical simulations of the solution the radially symmetric version of (6.1) with the results predicted by our analysis for axisymmetric traveling waves. Indeed, instability of the equilibrium solution is verified and the growing/decaying threshold behavior is apparent. Our result for the front position  $R(t)$ , (6.11), is shown to match the numerical simulations very well except when the solution collapses inward (and the large radius approximation cannot be expected to hold) and the structure of the front changes significantly. For the unstable growing solution, the front position is accurately given by (6.11) and in fact, since  $R(t)$  is increasing, we expect the accuracy of our approximation to steadily increase in time and the numerical solution should show convergence to the axisymmetric traveling wave.

The instability of the solutions smaller or larger than the critical nucleation front solution has been part of the focus of extensive studies in geometric models for the motion of diffusive interfaces (Fife [1988], Rubinstein et al. [1989]). In describing curved fronts in pattern forming reaction diffusion systems in mathematical biology, equation (6.10) is a prototype for unstable threshold behavior (Aronson and Weinberger [1978], Grindrod [1996]). Our solution of the axisymmetric problem for (6.1) is in fact just one special case of a more general theory for the motion of curved fronts in reaction-diffusion problems (Aronson and Weinberger [1978], Fife [1988], Jones [1983a], and [1983b], Kuzin and Pohozaev [1997], Nefedov [1993], Rubinstein and Sternberg [1992], Rubinstein et al. [1989], Terman [1987]). The general theory, as presented in these references and other works not cited here, characterizes all nonincreasing monotone radial solutions, shows that asymptotically

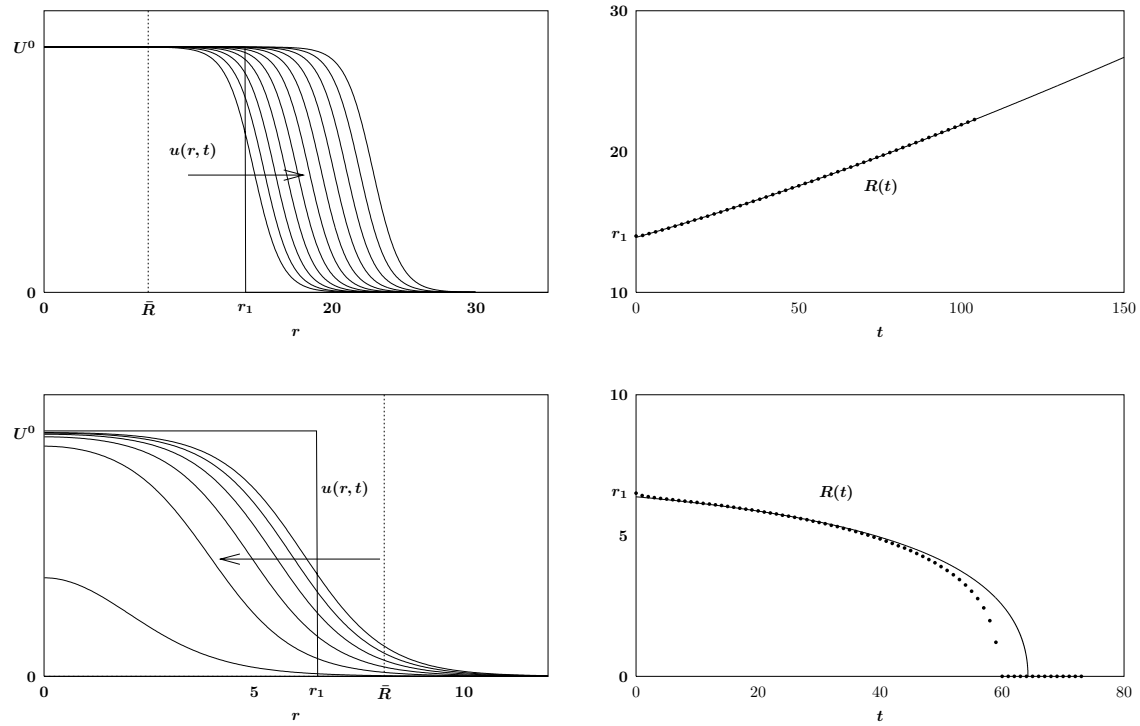


FIGURE 9. Numerical solutions of the radially symmetry reaction-diffusion equation (6.1) exhibiting nucleation threshold behavior. In both simulations the initial data is a step function  $u(r, 0) = u_0(r) = H(r - r_1)$ . Solution profiles at equally spaced times are shown (left) and the position of the front as a function of time (right). Solutions larger than the nucleation radius,  $r_1 > \bar{R}$ , will grow indefinitely (top). Solutions smaller than the nucleation radius,  $r_1 < \bar{R}$ , collapse inward (bottom).

along each ray expanding solutions approach planar wave fronts, and incorporates the effects of local curvature. Other general structures that can be described within this general theory include rotating spiral waves (Bernoff [1991], Murray [1990]) and more general helical waves (Grindrod [1996], Tyson and Keener [1988]). The results of these studies show that the speed of the motion of curved interfaces is given by the speed corresponding to one-dimensional planar interfaces, modified by corrections due to the mean curvature of the fronts. Recalling that the curvature is inversely proportional to the radius of curvature of a shape,  $\kappa = 1/R$ , we see that equation (6.9) is an example of this result,  $\tilde{c} = c(\omega) - (n - 1)\kappa$ . Numerous more advanced studies have derived this general result using locally orthogonal coordinate systems that are aligned with the dynamically evolving fronts. By contrast, in our presentation, we capture the leading order behavior using elementary applications of regular perturbation series and phase plane arguments.

**7. Transversal intersections of invariant manifolds and the heteroclinic orbits.** In this section we review some results from dynamical systems theory showing that the heteroclinic orbits found for  $c = c(\omega)$  in system (2.2) lie in the transverse intersections of certain invariant manifolds in the three-dimensional  $(U, V, c)$  phase space. This result, stated in subsection 7.2, demonstrates that the heteroclinic orbits are locally unique, and it is especially useful in establishing the stability of the solutions in the full partial differential equation. As a preliminary step in subsection 7.1, we study an earlier result that justifies the statements made in subsection 2.1 about the phase planes and the existence of a heteroclinic orbit at  $c = c(\omega)$ .

**7.1. Phase planes for  $\omega \in (\omega_{\min}, \omega_{\max})$  and  $c > 0$ .** In this subsection we will report on results for the equation (1.1) with  $c > 0$ . In particular, we show that, for each  $\omega \in (\omega_{\min}, \omega_{\max})$ , there exists a unique value of  $c = c(\omega)$  for which (1.1) has a ‘lower’ heteroclinic solution connecting  $(U^R, 0)$  to  $(U^L = 0, 0)$ . This demonstration then justifies the statements made in subsection 2.1 about the stable and unstable manifolds in this case.

The equation (1.1) may be written in system form as:

$$(7.1) \quad \begin{aligned} U' &= V \\ V' &= -cV - F(U; \omega). \end{aligned}$$

In order to follow the presentation of Fife [1979], we make the following coordinate change:  $\hat{V} = -V$ ,  $\hat{c} = -c$ , and  $\hat{z} = -z$ . This coordinate change makes  $\hat{c} < 0$  and transforms the ‘lower,’  $V < 0$ , heteroclinic solution connecting  $(U^R, 0)$  to  $(U^L = 0, 0)$  for (7.1) into an ‘upper,’  $V > 0$ , heteroclinic solution connecting  $(U^L, 0)$  to  $(U^R, 0)$  of the system

$$(7.2) \quad \begin{aligned} U' &= \hat{V} \\ \hat{V}' &= -\hat{c}\hat{V} - F(U; \omega). \end{aligned}$$

It is the existence of this upper connection that is established in Chapter 4.4 of Fife [1979], see the treatment there of ‘saddle-saddle connections,’ and we choose to follow this presentation for historical reasons, dropping hats from now on.

Let us examine the forward evolution under (7.2) of the trajectory on the upper right branch of the manifold  $W_{\text{loc}}^U(0, 0)$  with the parametrization chosen so that  $U(z = 0) = U^M$ . Since  $U$  is strictly increasing when  $V > 0$ , this trajectory must exit the semi-infinite strip  $0 \leq U \leq U^R$  and  $V \geq 0$  either through the  $U$ -axis with  $U \in (0, U^R)$  or through the line  $U = U^R$  with  $V > 0$ . Denote the exit point by  $(U_c, V_c)$ . Also, as in previous sections, it is useful to study the reformulation of (1.1) as a first-order equation for  $V$  as a function of  $U$ :

$$(7.31) \quad \frac{dV}{dU} + \frac{F(U; \omega)}{V} = -c.$$

The desired result is shown in three short steps. In step 1 it is shown that there exists a large negative value of  $c$  such that the solution of (7.3) with  $V(U = 0) = 0$  is a strictly increasing function on  $[0, U^R)$ . Hence,  $U_c = U^R$  and  $V_c > 0$ . Next, in step 2, we consider what happens as  $c$  increases from the large negative value found in step 1, showing that there exists a  $c_0$  such that  $V_{c_0} = 0$ , with either  $U_{c_0} = U^R$  or  $U_{c_0} < U^R$ . We remark that Step 2 is taken directly from part of a lemma due to Kanel, see Lemma 4.14 in Fife [1979]. Finally, in step 3, the possibility of  $U_{c_0} < U^R$  is ruled out for the nonlinear functions

$F(U; \omega)$  of the form studied in this article. Therefore, for the value of  $c_0$  found in step 2, it will be the case that  $U_{c_0} = U^R$ , so that the trajectory is precisely the heteroclinic connection to the saddle  $(U^R, 0)$  that was sought.

*Step 1.* Let us explicitly assume  $c < 0$  and that  $|c|$  is large. The proof will be by contradiction. Let us start by assuming that the conclusion is false, i.e., assume there exists a first maximum point  $(U_{\max}, V_{\max})$  with  $0 < U_{\max} < U^R$ . This maximum is given explicitly as

$$(7.4) \quad V_{\max} = -\frac{F(U_{\max}; \omega)}{c}.$$

On the one hand,  $V_{\max} > 0$ . Hence, (7.4) implies that  $F(U_{\max}; \omega) > 0$ , and from the properties of  $F$ , one therefore sees that  $U_{\max} > U^M$ . On the other hand, since  $F(U; \omega) < 0$  for  $U < U^M$ , one sees that  $dV/dU \geq -c$ . Hence, by integrating from  $U^L = 0$  to  $U^M$ , one finds

$$(7.5) \quad V(U^M) \geq |c|U^M,$$

since  $c < 0$ . Therefore, combining (7.4) and (7.5), it is seen that

$$|c|U^M \leq V_{\max} = \frac{F(U_{\max}; \omega)}{|c|},$$

which cannot be true for  $|c|$  large. This demonstrates, for  $c < 0$  and  $|c|$  large, that the solution along the local unstable manifold  $W_{\text{loc}}^U(U^L, 0)$  is a strictly increasing function for  $U \in (0, U^R)$ , and it completes step 1.

*Step 2.* Here we consider what happens for values of  $c$  less negative than those just obtained in step 1. The main work here is to compare two solutions  $V_1(U)$  and  $V_2(U)$  of (7.3), both with  $V = 0$  at  $U = U^L = 0$ , but such that  $c_1 > c_2$ . From (7.3), one directly gets

$$\frac{d}{dU}(V_1 - V_2) - \frac{F(U; \omega)}{V_1 V_2}(V_1 - V_2) = -(c_1 - c_2).$$

Introducing an integrating factor, this equation may be rewritten as:

$$(7.6) \quad \begin{aligned} & \frac{d}{dU}[(V_1 - V_2)Z(U)] = -(c_1 - c_2)Z(U) \\ Z(U) = \exp \left\{ - \int_{U^M/2}^U \left( \frac{F(U'; \omega)}{V_1(U')V_2(U')} \right) dU' \right\}. \end{aligned}$$

The lower limit in the integrating factor was taken to be  $U^M/2$  here for definiteness. Now, as  $U \rightarrow 0^+$ , the difference  $(V_1 - V_2)$  vanishes, while the exponential factor stays bounded since  $F < 0$  and the integration is from right to left. Hence, the term in square brackets also vanishes in the limit. Finally, we observe that this term in square brackets is a strictly decreasing function by (7.6), since  $c_1 - c_2 > 0$ ; and, therefore,  $V_1(U) - V_2(U)$  must approach zero from below.

The above estimate establishes the desired comparison result:  $c_1 > c_2$  implies  $V_1(U) < V_2(U)$  for  $U > 0$  along the trajectories on  $W_{\text{loc}}^U(0, 0)$ . If one increases the value of  $c$  from that obtained in step 1 (i.e., one takes a sequence of less negative values), then the graphs of the functions  $V(U)$  giving these manifolds form a monotonically decreasing sequence of curves, and there exists a value of  $c$ , call it  $c_0$ , such that  $V_{c_0} = 0$ .

*Step 3.* Here we rule out the possibility that  $U_{c_0} < U^R$ . This will imply that  $U_{c_0} = U^R$ , so that in the system with the value  $c_0$  just obtained in step 2, the manifold  $W_{\text{loc}}^U(0, 0)$  coincides with the manifold  $W_{\text{loc}}^S(U^R, 0)$ , i.e., there is an upper heteroclinic connection from  $(0, 0)$  to the other saddle at  $(U^R, 0)$ , as desired.

If  $U_{c_0} < U^R$ , then the trajectory on  $W_{\text{loc}}^U(0, 0)$  crosses the  $U$ -axis with a vertical tangent at  $(U_{c_0}, 0)$ . Hence, the manifold  $W_{\text{loc}}^U(0, 0)$  obtained for the system with  $c$  slightly less than  $c_0$  will have zero slope at more than one point to the left of  $(U^R, 0)$ , i.e.,  $dV/dU$  will have two roots  $U_1, U_2 < U^R$ . One can then readily show that this implies that  $F(U; \omega)$  has an additional root less than  $U^R$  and not equal to  $U^M$ , which contradicts our assumptions about  $F$ .

This completes the proof of the existence of a value of  $c_0 = c(\omega)$  for which (1.1) has an upper heteroclinic orbit for each  $\omega \in (\omega_{\min}, \omega_{\max})$ , as stated in subsection 2.1.

**7.2. Transversality for (2.2) in  $(U, V, c)$  space.** In this subsection we review well-known results, see Jones [1995], Jones et al. [1991], showing that the heteroclinic orbit of (1.1) studied above for  $c > 0$  lies in the transverse intersection of two invariant manifolds in the three-dimensional  $(U, V, c)$  phase space. As a consequence, the heteroclinic orbit will be locally unique. Also, this transversality is important for demonstrating stability of traveling waves in the full reaction diffusion partial differential equations, see Jones [1984].

For each  $\omega \in (\omega_{\min}, \omega_{\max})$ , we will analyze the sequence of  $(U, V)$  phase planes obtained in sections 2.1 and 7.1 for  $c \in (c(\omega) - \delta, c(\omega) + \delta)$ , where  $\delta > 0$  is fixed, in the three-dimensional  $(U, V, c)$  space. Let  $\mathcal{L} = \{(U^L(c), 0, c) | c \in (c(\omega) - \delta, c(\omega) + \delta)\}$ , and  $\mathcal{R} = \{(U^R(c), 0, c) | c \in (c(\omega) - \delta, c(\omega) + \delta)\}$ , for a fixed  $\delta > 0$ . Now, one directly obtains two-dimensional surfaces (manifolds) by taking the unions over  $c$  of the local stable and unstable manifolds of the saddle equilibria obtained for each individual  $c$ . For example,  $W_{\text{loc}}^U(\mathcal{R}) \equiv \cup_{c \in (c(\omega) - \delta, c(\omega) + \delta)} W_{\text{loc}}^U(U^R(c), 0)$ . At each point on both of these manifolds, the tangent spaces are two-dimensional, and we recall that two surfaces (manifolds) in  $\mathbf{R}^3$  are said to intersect each other transversely at a point if the sum of the dimensions of their tangent spaces at that point is three. We show in this subsection that, for each fixed value of  $\omega \in (\omega_{\min}, \omega_{\max})$ , the two surfaces  $W_{\text{loc}}^U(\mathcal{R})$  and  $W_{\text{loc}}^S(\mathcal{L})$  intersect each other transversely in the three-dimensional  $(U, V, c)$  space precisely along the one-dimensional heteroclinic orbit in the  $c = c(\omega)$  plane. The results stated here are taken directly from Section 4.5 of Jones [1995], with only minor modifications to adapt the argument to the lower heteroclinic orbit from  $(U^R, 0)$  to  $(0, 0)$  studied here, and to use vectors as opposed to differential forms.

We will use the notation  $\eta_1^\pm \equiv (\Delta U_1^\pm, \Delta V_1^\pm, \Delta c_1^\pm)$  and  $\eta_2^\pm \equiv (\Delta U_2^\pm, \Delta V_2^\pm, \Delta c_2^\pm)$ , to denote two independent vectors on the tangent plane to a stable manifold (+) or an unstable manifold (-). A normal vector,  $\mathbf{n}$ , to such a tangent plane is obtained by taking cross-products of  $\eta_1$  and  $\eta_2$ :

$$\begin{aligned} \mathbf{n} &= (n_1, n_2, n_3) \\ &= (\Delta V_1 \Delta c_2 - \Delta c_1 \Delta V_2, -\Delta U_1 \Delta c_2 + \Delta U_2 \Delta c_1, \Delta U_1 \Delta V_2 - \Delta V_1 \Delta U_2). \end{aligned}$$

In addition, we will need to have a convenient way in which to measure the distance between the manifolds  $W^U(U^R, 0)$  and  $W^S(0, 0)$ , as well as the rate at which that distance changes as  $c$  changes. Hence, we follow Jones [1995] and, for fixed  $\omega \in (\omega_{\min}, \omega_{\max})$ , define  $h^\mp(c)$  to be the points at which the manifolds  $W^U(U^R, 0)$  and  $W^S(0, 0)$ , respectively, intersect the vertical line  $U = U^M$  in the  $(U, V)$  plane. On the  $c = c(\omega)$  plane, this distance will be zero, since the manifolds coincide there. We will be interested in the rates at which  $h^\mp(c)$  change as  $c$  changes through  $c(\omega)$ , and in particular to show that

$$(7.7) \quad \left( \frac{\partial h^-}{\partial c} - \frac{\partial h^+}{\partial c} \right) \Big|_{c=c(\omega)} \neq 0.$$

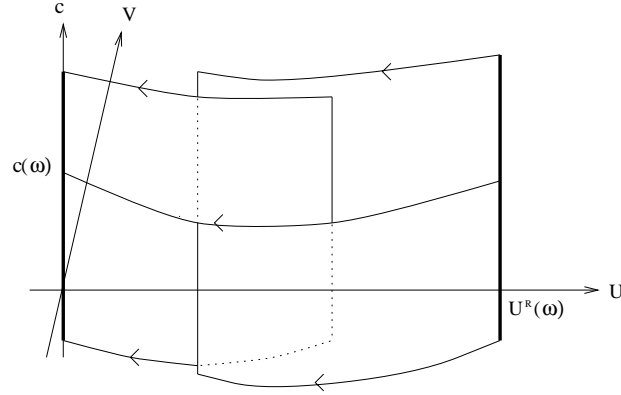


FIGURE 10. Schematic picture of transversal intersection of the unstable and stable manifolds in  $(U, V, c)$  phase space. The thick solid curves are  $\mathcal{L}$  and  $\mathcal{R}$ , and they depend on  $\omega$ .

When this inequality holds, the manifolds transversely intersect in the three-dimensional  $(U, V, c)$  space.

The evolution of the components of the tangent and normal vectors is determined directly from the equation of variations, see, e.g., Coddington and Levinson [1987]. For (2.2) with the equation  $c' = 0$  appended, we find:

$$\begin{aligned}
 \Delta U' &= \Delta V \\
 (7.8) \quad \Delta V' &= -c\Delta V - V(z)\Delta c - f'(U(z))\Delta U + \omega\Delta U \\
 \Delta c' &= 0.
 \end{aligned}$$

Here, the terms  $U(z)$  and  $V(z)$  are evaluated along the heteroclinic orbit for  $c = c(\omega)$ , and the quantities  $\Delta U$ ,  $\Delta V$ ,  $\Delta c$  denote the variations in the  $U$ ,  $V$ , and  $c$  variables from their values along that heteroclinic orbit. Starting from the definition of  $\mathbf{n}$  and using the chain rule derivative, we find:

$$\begin{aligned}
 (7.9) \quad n_1' &= -cn_1 + (f'(U) - \omega)n_2 \\
 n_2' &= -n_1 \\
 n_3' &= V(z)n_2 - cn_3.
 \end{aligned}$$

We shall only need the  $n_3$  equation.

Having set up all of the general theory, we now make a specific choice, following the judicious selection in Jones [1995], Jones et al. [1991], of the two vectors in the tangent planes:

$$\begin{aligned} \eta_1^\pm &\equiv (\Delta U_1^\pm, \Delta V_1^\pm, \Delta c_1^\pm) = \left(0, \frac{\partial h^\pm}{\partial c}, 1\right) \\ \eta_2 &\equiv (\Delta U_2^\pm, \Delta V_2^\pm, \Delta c_2^\pm) = (V, -cV - F(U; \omega), 0). \end{aligned}$$

Of course, by selecting the vector field of the original system (2.2) as the second vector, the vector  $\eta_2$  is the same on the tangent planes to both manifolds. Therefore, we see by explicit calculation that, for this choice,  $n_1(z) = cV(z) + F(U(z); \omega)$ ,  $n_2(z) = V(z)$ , and

$$(7.10) \quad n_3(0) = -V(z=0)(\partial h^\pm / \partial c).$$

The first two components are known for all  $z$ , since the vector field and heteroclinic solution  $(U(z), V(z))$  are functions of  $z$ , whereas the terms  $\partial h^\pm / \partial c$  are only defined on the line  $U = U^M$  (i.e., at  $z = 0$ ), so that  $n_3$  is known so far only in terms of the unknown derivatives of  $h$  and only at  $z = 0$ .

From (7.9), we now have the explicit differential equation for  $n_3(z)$ :

$$(7.11) \quad n_3' = -cn_3 + V(z)^2.$$

This equation may be solved along each of the manifolds in terms of  $V(z)$  with the aid of an integrating factor, and by integrating along  $W^U(U^R, 0)$  we get:  $n_3(z) = e^{-cz} \int_{-\infty}^z V(z')^2 e^{cz'} dz'$ . Hence, we immediately obtain:

$$(7.12) \quad n_3(0) = \int_{-\infty}^0 V(z')^2 e^{cz'} dz' > 0.$$

By combining (7.10) and (7.12) and because  $V < 0$  along the heteroclinic orbit, we get

$$(7.13) \quad \left. \frac{\partial h^-}{\partial c} \right|_{c=c(\omega)} > 0.$$

Now, in precisely the same fashion, one can show that

$$(7.14) \quad \left. \frac{\partial h^+}{\partial c} \right|_{c=c(\omega)} < 0.$$

Hence, combining (7.13) and (7.14), one obtains the desired result:

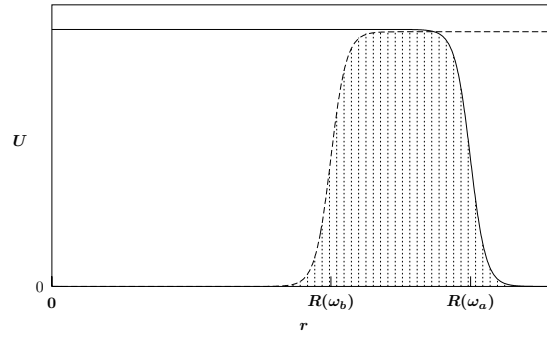
$$(7.15) \quad \left( \frac{\partial h^-}{\partial c} - \frac{\partial h^+}{\partial c} \right) \Big|_{c=c(\omega)} > 0,$$

and the proof of transversality is complete.

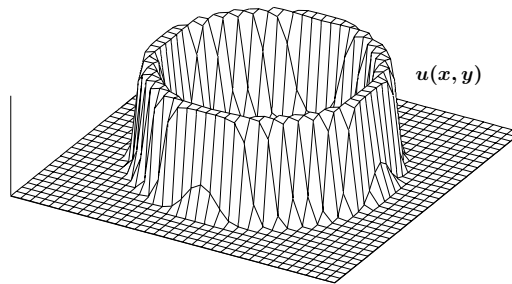
**8. Discussion.** In this article we have reviewed how a combination of phase plane analysis and perturbation methods can be used to obtain radially symmetric solutions of semilinear elliptic equation and reaction-diffusion systems. By treating the nonautonomous coefficients in the radial differential equation as slowly varying parameters, we were able to obtain an asymptotically accurate autonomous solution from the phase plane solution of the damped equation (1.1). Use of a family of exact solutions for the autonomous problem proved very helpful in the analysis of the problem and in the examination of general properties of the radial solutions.

We also reviewed the demonstration due to Jones [1995], Jones et al. [1991] that the heteroclinic orbit of (2.2) lies in the transverse intersection of the stable and unstable manifolds of equilibria in the full three-dimensional  $(U, V, c)$  phase space, precisely in the plane  $c = c(\omega)$ . This result directly implied the local uniqueness of the heteroclinic orbit. It is hoped that our review of this result for traveling waves in one-space dimension, or planar interfaces in higher space dimensions, will motivate the reader to study the more advanced results derived for curved fronts in axisymmetric higher-dimensional problems,  $n > 1$ . In the papers by Aronson and Weinberger [1978], Atkinson and Peletier [1986], Berestycki and Lions [1980], Brezis and Lieb [1984], and Jones [1983b], the existence and local uniqueness of radially decreasing solutions are demonstrated for the nonautonomous problems (1.10). These results are more general than that obtained here via perturbation methods, since no large interface assumptions are made. Moreover, the existence of a threshold effect (recall Section 6) is established in a much more general context than that shown here, and it is proven that asymptotically, along every ray emanating from the origin in the  $n$ -dimensional space, the shapes of the solutions approach that of the one-dimensional traveling wave, see Aronson and Weinberger [1978], Jones [1983b].

A careful review of our approach suggests methods for use of the interface solutions to construct more general geometric structures, or



(a)



(b)

FIGURE 11. Construction of the pulse from increasing and decreasing front solutions with  $R = R(\omega_a)$  and  $R = R(\omega_b)$  (a), and a three-dimensional representation of the corresponding annular ring solution.

more general nonautonomous equations of the form

$$(8.1) \quad \frac{d^2U}{dr^2} + G(r)\frac{dU}{dr} + F(U; \omega(r)) = 0.$$

A classical perturbation expansion of the interface structure begins with the leading order problem of a stationary planar front. This is an interface with zero curvature, or equivalently, an infinite radius of curvature,  $R \rightarrow \infty$ . The interface structure is given by the lower heteroclinic orbit in the Hamiltonian phase plane shown in Figure 4b with  $\omega = \omega_0$ . While zero curvature is maintained, the governing differential equation (1.1) is autonomous and the solution has translation invariance. When the front has any finite amount of curvature, translation

invariance is lost, as in the nonautonomous equation (4.1), and the Hamiltonian structure is lost due to the introduction of a slowly varying damping term. We have constructed monotone decreasing solutions for this case, in the range  $\omega_{\min} < \omega < \omega_0$ . However, we noted from the phase plane analysis of the damped equation (2.1) that heteroclinic orbits, corresponding to interface solutions, exist in a larger range, for all  $\omega_{\min} < \omega < \omega_{\max}$ . Earlier, the solutions for  $\omega_0 < \omega < \omega_{\max}$  were dismissed as representing unphysical solutions with a negative damping coefficient,  $c < 0$ , describing a negative radial position,  $R < 0$ . However, using the invariance of equation (2.1) under the transformation  $z \rightarrow -z$  and  $c \rightarrow -c$ , these solutions can be shown to describe monotone *increasing* fronts with a positive radial position. For the family of problems with closed-form solutions described in Section 2.1, these results are given by

$$(8.2) \quad \begin{aligned} U(z) &= \frac{U^R}{[1 + (U^R)^k \exp\{-k(U^R)^k(z - z_0)\}]^{1/k}}, \\ c(\omega) &= \frac{\omega}{U^R(\omega)^k} - U^R(\omega), \end{aligned}$$

for  $\omega \in (\omega_0, \omega_{\max})$ , and the radial position is still given by (4.2),  $R = (n - 1)/c(\omega) > 0$ . The radial position for these increasing fronts is plotted in Figure 8 for  $\omega > \omega_0$ . For  $\omega \searrow \omega_0$  this branch of solutions is the finite damping continuation of the *upper* heteroclinic orbit from the Hamiltonian phase plane system.

Using these observations, it becomes clear how to construct annular ring solutions, the radially symmetric analogue of one-dimensional pulse solutions. If the parameter  $\omega$  is allowed to slowly vary from above  $\omega_0$  to below  $\omega_0$  as  $r$  increases then the increasing and decreasing fronts can be used to form a localized pulse. For example if  $\omega(r)$  is given by

$$(8.3) \quad \omega(r) = \frac{1}{2}(\omega_a + \omega_b) + \frac{1}{2}(\omega_b - \omega_a) \tanh\left(\frac{r - r_0}{\delta}\right),$$

with  $\delta \ll r_0$  and  $\omega_b > \omega_0 > \omega_a$  then  $\omega \sim \omega_a$  for  $r < r_0$  and  $\omega \sim \omega_b$  for  $r > r_0$ . This form of  $\omega(r)$  was used to construct the annular solution shown in Figure 11. While equation (8.3) gives an arbitrary form for  $\omega(r)$ , we can imagine this front-like solution coming from another semilinear elliptic equation that couples  $\omega(r)$  to  $U(r)$ , and similarly

for a time-dependent system of reaction-diffusion equations like the FitzHugh-Nagumo model. Other forms of  $\omega(r)$  coupled to our equation for  $u$ , (6.1) could give periodic trains of axisymmetric pulses; these are often called “target patterns” (Murray [1990]). Similarly, a weak dependence on a variation in the angular direction,  $\omega = \omega(r, \theta)$  would perturb such solutions to produce spiral wave patterns (Bernoff [1991]) from these rings.

**Acknowledgments.** TW thanks Thomas Beale, Andrew Bernoff, Robert Almgren and Radica Sipcic for helpful discussions. TK gratefully acknowledges support from an Alfred P. Sloan Fellowship and an NSF CAREER award.

#### REFERENCES

- M. Abramowitz and I.A. Stegun [1965], *Handbook of Mathematical Functions*, Dover, New York.
- D.W. Aronson and H.F. Weinberger [1978], *Multidimensional Nonlinear Diffusion Arising in Population Genetics*, Adv. Math. **30**,
- F.V. Atkinson and L.A. Peletier [1986], *Ground States of  $-\Delta u = f(u)$  and the Emden-Fowler Equation*, Arch. Rational Mech. Anal. **93**, 103–127.
- P.W. Bates and P.C. Fife [1993], *The Dynamics of Nucleation for the Cahn-Hilliard Equation*, SIAM J. Appl. Math. **53**, 990–1008.
- C.M. Bender and S.A. Orszag [1978], *Advanced Mathematical Methods for Scientists and Engineers*, McGraw-Hill, New York.
- R.D. Benguria and M.C. Depassier [1994], *New Exact Fronts for the Nonlinear Diffusion Equation with Quintic Nonlinearities*, preprint.
- H. Berestycki and P.L. Lions [1980], *Existence of Stationary States in Nonlinear Scalar Field Equations*, in *Bifurcation Phenomena in Mathematical Physics and Related Topics* (C. Bardos and D. Bessis, eds.), Reidel.
- A.J. Bernoff [1991], *Spiral Wave Solutions for Reaction-Diffusion Equations in a Fast Reaction/Slow Diffusion Limit*, Phys. D **53**, 125–150.
- D. Borgis and M. Moreau [1988], *Nucleation Theory for a Model Bistable Chemical Reaction*, J. Statist. Phys. **50**, 935–962.
- H. Brezis and E.H. Lieb [1984], *Minimum Action Solutions of Some Vector Field Equations*, Comm. Math. Phys. **96**, 97–113.
- G. Caginalp [1991], *Phase Field Models and Sharp Interface Limits: Some Differences in Subtle Situations*, Rocky Mountain J. Math. **21**, 603–615.
- S.-K. Chan [1977], *Steady-State Kinetics of Diffusionless First Order Phase Transformations*, J. Chem. Phys. **67**, 5755.

- S. Chen and G. Lu [1997], *Asymptotic Behavior of Radial Solutions for a Class of Semilinear Elliptic Equations*, J. Differential Equations **133**, 24–254.
- J. Cisternas and M.C. Depassier [1996], *On a Conjecture of Goriely for the Speed of Fronts of the Reaction-Diffusion Equation*, preprint.
- E.A. Coddington and N. Levinson [1987], *Theory of Ordinary Differential Equations*, reprinted ed., Krieger, Malabar, FL.
- J.M. Dixon, J.A. Tuszynski and M. Otwinowski [1991], *Special Analytical Solutions of the Damped Anharmonic Oscillator Equation*, Phys. Rev. A **44**, 3484–3491.
- P.C. Fife [1979], *Mathematical Aspects of Reacting and Diffusing Systems*, Lecture Notes in Biomath. **28**, Springer-Verlag, Berlin.
- P.C. Fife [1988], *Dynamics of Internal Layers and Diffusive Interfaces*, CBMS-NSF Regional Conf. Ser. in Appl. Math. bf53, SIAM, Philadelphia.
- P.C. Fife and J.B. McLeod [1981], *A Phase Plane Discussion of Convergence to Traveling Fronts for Nonlinear Diffusion*, Arch. Rational Mech. Analysis **75**, 281–314.
- B. Friedman [1990], *Principles and Techniques of Applied Mathematics*, Dover, New York.
- B. Gidas, W.-M. Ni and L. Nirenberg [1979], *Symmetry and Related Properties via the Maximum Principle*, Comm. Pure Appl. Math. **68**, 209–243.
- H. Goldstein [1980], *Classical Mechanics*, 2nd ed., Addison-Wesley, Reading, MA.
- R.E. Goldstein, D.J. Muraki and Dean M. Petrich [1996], *Interface Proliferation and the Growth of Labyrinths in a Reaction-Diffusion System*, Phys. Rev. E **53**, 3933–3957.
- A. Goriely [1995], *Simple Solution to the Nonlinear Front Problem*, Phys. Rev. Lett. **75**, 2047–2050.
- P. Grindrod [1996], *The Theory and Applications of Reaction-Diffusion Equations*, Clarendon Press, Oxford.
- J. Guckenheimer and P. Holmes [1983], *Nonlinear Oscillations, Dynamical Systems, and Bifurcations of Vector Fields*, Springer-Verlag, New York.
- C.K.R.T. Jones [1983a], *Asymptotic Behavior of a Reaction-Diffusion Equation in Higher Space Dimensions*, Rocky Mountain J. Math. **13**, 355–364.
- C.K.R.T. Jones [1983b], *Spherically Symmetric Solutions of a Reaction-Diffusion Equation*, J. Differential Equations **49**, 142–169.
- C.K.R.T. Jones [1984], *Stability of the Traveling Wave Solution of the FitzHugh-Nagumo System*, Trans. Amer. Math. Soc. **286**, 431–469.
- C.K.R.T. Jones [1989], *Geometric Singular Perturbation Theory*, in *Dynamical Systems, Montecatini Terme* (R. Johnson, ed.), Lecture Notes in Math. **1609**, Springer-Verlag, Berlin, 44–118.
- C.K.R.T. Jones, N. Kopell and R. Langer [1991], *Construction of the FitzHugh-Nagumo Pulse Using Differential Forms*, in *Patterns and Dynamics in Reactive Media* (H. Swinney, G. Aris and D. Aronson, eds.), IMA Vol. Math. Appl. **37** Springer-Verlag, New York, 101–116.

- H.G. Kaper and M.K. Kwong [1988], *Uniqueness of Nonnegative Solutions of a Class of Semi-Linear Elliptic Equations*, in *Nonlinear Diffusion Equations and Their Equilibrium States II* (W.-M. Ni, L.A. Peletier and J. Serrin, eds.), Springer-Verlag, New York.
- J. Keener and J. Sneyd [1998], *Mathematical Physiology*, Springer-Verlag, New York.
- B.S. Kerner and V.V. Osipov [1994], *Autosolitons: A New Approach to Problems of Self-Organization and Turbulence*, Kluwer Academic, Dordrecht.
- J.K. Kevorkian and J.D. Cole [1996], *Multiple Scales and Singular Perturbation Methods*, Springer-Verlag, New York, 1996.
- I. Kuzin and S. Pohozaev [1997], *Entire Solutions of Semilinear Elliptic Equations*, Birkhauser, Basel, 1997.
- H. Lamb [1993], *Hydrodynamics*, Cambridge University, Cambridge.
- L. Lewin [1981], *Polylogarithms and Associated Functions*, North-Holland, New York.
- M. Lifschitz and K.F. Freed [1993], *Interfacial Behavior of the Compressible Polymer Blends*, J. Chem. Phys. **98**, 8994–9013.
- A.J. Majda and A.L. Bertozzi [1999], *Vorticity and the Mathematical Theory of Incompressible Fluid Flow*, Cambridge University, Cambridge.
- H.P. McKean [1970], *Nagumo's Equation*, Adv. in Math. **vol. no?**, 209–223.
- J.B. McLeod and J. Serrin [1968], *The Existence of Similarity Solutions for Some Laminar Boundary Layer Problems*, Arch. Rational Mech. Anal. **36**, 288–303.
- K. McLeod and J. Serrin [1987], *Uniqueness of Positive Radial Solutions of  $\Delta u + f(u) = 0$  in  $R^n$* , Arch. Rational Mech. Anal. **99**, 115–145.
- J.D. Murray [1990], *Mathematical Biology*, Springer-Verlag, Berlin.
- N.N. Nefedov [1993], *Contrast Structures of Spike Type in Nonlinear Singularly Perturbed Elliptic Equations*, Dokl. Math. **46**, 410–413.
- W.-M. Ni [1988], *Some Aspects of Semilinear Elliptic Equations in  $R^n$* , in *Nonlinear Diffusion Equations and Their Equilibrium States II* (W.-M. Ni, L.A. Peletier and J. Serrin, eds.), Springer-Verlag, New York.
- R.L. Pego [1989], *Front Migration in the Nonlinear Cahn-Hilliard Equation*, Proc. Roy. Soc. London Ser. A **422**, 261–278.
- J.A. Powell [1997], *Conditional Stability of Front Solutions*, J. Math. Biol. **35**, 729–747.
- J.A. Powell and M. Tabor [1992], *Non-Generic Connections Corresponding to Front Solutions*, J. Phys. A. **25**, 3773–3796.
- S. Puri and K. Binder [1991], *Phenomenological Theory for the Formation of Interfaces via the Interdiffusion of Layers*, Phys. Rev. B **44**, 9735–9738.
- J. Rubinstein and P. Sternberg [1992], *Nonlocal Reaction-Diffusion Equations and Nucleation*, IMA J. Appl. Math. **48**, 249–264.
- J. Rubinstein, P. Sternberg and J.B. Keller [1989], *Fast Reaction, Slow Diffusion, and Curve Shortening*, SIAM J. Appl. Math. **49**, 116–133.
- J.E. Taylor and J.W. Cahn [1994], *Linking Anisotropic Sharp and Diffuse Surface Motion Laws via Gradient Flows*, J. Statist. Phys. **77**, 183–197.

- D. Terman [1987], *Infinitely Many Radial Solutions of an Elliptic System*, Ann. Inst. H. Poincaré Anal. Non Linéaire. **4**, 549–604.
- D. Terman [1988], *Connection Problems Arising from Nonlinear Diffusion Equations*, in *Nonlinear Diffusion Equations and Their Equilibrium States II* (W.-M. Ni, L.A. Peletier and J. Serrin, eds.), Springer-Verlag, New York, 315–332.
- J.J. Tyson and J.P. Keener [1988], *Singular Perturbation Theory of Traveling Waves in Excitable Media*, Phys. D **32**, 327–361.
- A.B. Vasil'eva, V.F. Butuzov and L.V. Kalachev [1995], *The Boundary Function Method for Singularly Perturbed Problems*, SIAM, Philadelphia.
- A.I. Volpert, V.A. Volpert and V.A. Volpert [1994], *Traveling Wave Solutions of Parabolic Systems*, Amer. Math. Soc., Providence, RI.
- T.P. Witelski [1996], *The Structure of Internal Layers for Unstable Nonlinear Diffusion Equations*, Stud. Appl. Math. **96**, 277–300.
- T.P. Witelski [1998], *Equilibrium Interface Solutions of a Degenerate Singular Cahn-Hilliard Equation*, Appl. Math. Lett. **11**, 127–133.
- T.P. Witelski, A.Yu. Grosberg and T. Tanaka [1998], *On the Properties of Polymer Globules in the High Density Limit*, J. Chem. Phys. **108**, 9144–9149.
- T.P. Witelski, K. Ono and T.J. Kaper [1998], *Analysis of the Critical Wave Speeds of Scalar Reaction-Diffusion Equations*, Appl. Math. Lett., submitted; also available as Tech. Rep. 5, Boston Univer., Center for BioDynamics, April, 1998.